HTI 89TR16

HPOCS 23-1

Pressure Oxygen Compressor
(HPOCS) Development Program

Final Report
Requirement No. 23

Contract NAS-9-18005

February 28, 1989

CORPORATED
Road
York 12110

MTI 89TR16

HPOCS 23-1

HIGH PRESSURE OXYGEN COMPRESSOR SYSTEM (HPOCS) DEVELOPMENT PROGRAM

DATA REQUIREMENT NO. 23
TASK I FINAL REPORT

February 28, 1989

Prepared Under Contract
NAS-9-18005

for

NASA Lyndon B. Johnson Space Center
Space and Life Sciences Procurement Branch
Houston, Texas 77053

Prepared by: W.D. Waldron
Program Manager

Approved by: N. Nightingale
Manager, Stirling Engine Systems Division

MECHANICAL TECHNOLOGY INCORPORATED
968 Albany-Shaker Road
Latham, New York 12110

TABLE OF CONTENTS

LIST OF FIGURES

LIST OF TABLES

1.0 INTRODUCTION AND SUMMARY

1.1 Program Objectives and Basic Approach

This report describes the results of Task 1.0 of the High Pressure Oxygen Compressor System (HPOCS) Development Program conducted for NASA-JSC under Contract NAS-9-18005. Task 1.0 is entitled "HPOCS Charge Rate Study".

The overall program objectives are to design, fabricate, and test an engineering prototype High Pressure Oxygen Compressor System (HPOCS) suitable for recharging the high pressure oxygen tanks in a space station Extravehicular Mobility Unit (EMU) life support system.

The objectives of the Task 1.0 charge rate study are to:

1. Determine optimal HPOCS charge rate that will provide one hour reservicing capability for two EMU's (at 5.91 lbs high pressure oxygen each).

2. Determine advantages and disadvantages of directly recharging EMU tanks vs. using accumulators to charge tanks.

The optimal HPOCS charge rate to be based upon:

Minimization of: Size
Weight
Power Consumption

Maximization of: Safety
Reliability
Life

The term EMU refers to the "Extravehicular Mobility Unit" which is basically the space suit including all life support systems that the astronaut requires while outside the space station environment. Each space station air-lock supports two EMU's and the subject HPOCS services both EMU's.

Within the EMU is the Portable Life Support System (PLSS). Each PLSS consists of two oxygen tanks capable of holding 2.955 lbs of gaseous oxygen at 6000 psia. Thus, the total charge that must be provided by the HPOCS is 11.82 lbs. The terms EMU and PLSS are used interchangeably in this report.

The contract work statement defines the HPOCS charge rate study in the following words:

> The trade study shall be performed by the contractor to determine the optimum charge rate for the HPOCS that will provide a one hour reservicing capability for two EMU's (each EMU requires 5.91 lbs of oxygen for a complete recharge). The range of the charge rate the contractor shall investigate is from 0.75 to 11.82 lbs/hr. The study shall determine the advantages and disadvantages of directly recharging the EMU oxygen tanks with the HPOCS or charging the EMU oxygen tanks using the HPOCS with accumulators. In determining the charge rate, the contractor shall take into account at least the following factors: power requirements, technology risk, complexity, maintainability, safety, and size and weight of accumulators.

Early in the program, the NASA-JSC Technical Manager, recognizing that the oxygen consumed during a normal EVA (Extravehicular Activity) mission would be but a fraction of the total inventory of 11.82 lbs, requested that the study efforts concentrate on reservicing charges of less than 11.82 lbs. Based upon his input, the "normal" usage per EVA mission was established as 2.955 lbs for the two EMU's.

To establish the basic data required to accomplish the objectives of the HPOCS charge rate study task, preliminary designs were established for three different compressor sizes, i.e. 0.75, 6.0, and 11.82 lb/hr at 6000 psia discharge pressure. In addition, two designs were prepared for the 6.0 lb/hr machine (one operating at 25 Hz, and one at 32 Hz). For the accumulator charge approach, three different accumulator sizes were considered, i.e. 0.1751, 0.3502, and 0.8755 ft^3.

The optimum charge rate (compressor size), recharge time, and accumulator size/usage conclusions were based upon the total cost to launch the compressor and accumulators (in terms of cost per pound) and the cost of compressor energy usage over the 30 year life cycle. The cost basics suggested by the NASA-JSC Technical Manager were $4000/lb for launch and $0.15/watt-hr for energy consumption.

1.2 Summary of Results and Conclusions

The conclusions of the HPOCS charge rate study are:

- From a cost standpoint, weight is more significant than energy consumption
- The direct charge approach results in minimum weight and energy consumption, and thus, minimum launch and 30 year energy consumption cost
- The optimum charge time for a 2.955 lb direct recharge is 0.6 hours (based upon minimization of weight and energy consumption)
- The optimum compressor size based upon minimization of weight is approximately 4 lbs/hr (this size produces the 2.955 lb direct recharge in 0.6 hours)
- A 4 lb/hr compressor will recharge (in the direct charge mode) the total inventory of 11.82 lb in approximately 2.2 hours. A 10 lb/hr compressor is required to recharge the 11.82 lbs in 1 hour.
- The peak power consumed by a 4 lb/hr compressor is approximately 360 watts. Its energy consumption for the 2.955 lb and 11.82 lb recharge cycles is approximately 230 w-hr and 715 w-hr respectively.
- Compressor size, per se, has little effect on compressor safety, reliability, and life issues
- The accumulator charge approach:

- Allows for a partial recharge cycle without compressor operation

- Increases system complexity and the quantity of stored high pressure oxygen

- Results in more thermal energy transfer considerations because of the requirement for accumulator reheat

• A second compressor may be more weight-effective than accumulators to increase system reliability (the second compressor provides redundancy)

1.3 Recommendations

Based upon the foregoing results and conclusions, the following recommendations relative to the study objectives are:

1. Optimize the compressor design at 4 lb/hr based upon weight and energy minimization

2. Select direct charge approach because it minimizes total system weight

1.4 Report Organization

The remainder of this report is divided into five major sections.

Section 2.0 expands upon the specification requirements and describes the overall engineering preprototype HPOCS system.

In Section 3.0, the basic compressor operation and construction are described along with the basic design criteria imposed for the purpose of this study.

The approach to sizing each of the four compressor assemblies is discussed in Section 4.0. This section concludes with the basic performance of each of the compressors in terms of flow rate and power consumption as functions of discharge pressure.

In Section 5.0, the various aspects of charging the PLSS tanks either directly or with the different size accumulators are addressed. For all situations covered in Section 5.0, isothermal charging is assumed.

Section 6.0 considers the aspects of nonisothermal charging in terms of temperature, pressure, and energy transfer, and how accumulator size influences these aspects.

2.0 SPECIFICATION REQUIREMENTS AND ENGINEERING PREPROTOTYPE SYSTEM DESCRIPTION

2.1 HPOCS Design Conditions

The design requirements for the HPOCS stated in Section 3.1 of the contract Statement of Work are restated here for reference in subsequent sections of this technical discussion.

HPOCS Design Conditions

Inlet Pressure	200 psia
Inlet Temperature	70°F
Inlet Dew Point Temperature	58°F
Discharge Pressure	6000 psia
Discharge Temperature	70°F
Discharge Dew Point Temperature	20.5°F
Average Continuous Power Goal	100 W max

The average continuous power of 100 watts maximum, if interpreted to mean the average power to pump the 11.82 lb charge from 200 psia to 6000 psia in one hour is a physical impossibility. If one were to assume 100% efficient adiabatic compression in two stages with perfect inter-cooling and no motor or transmission losses (100% electrical and mechanical efficiency), the power required at the final discharge pressure would be 499 watts (see Appendix A), and the average power will far exceed 100 watts.

Amendment 1A to the RFP clarifies the 100 watt goal by stating ..."The 100 watt average continuous power requirement is a goal, not a requirement. The 100 watt average continuous power goal relates to the duty cycle in that it is a goal that the compressor does not exceed 100 watts if operated continuously; or in a 24 hour period, the power needed does not exceed 2400 watts."

Based upon this clarification, it was assumed that the maximum energy consumption goal was to be less than 2400 watt-hours for an 11.82 lb charge cycle pumped

from 200 psia to 6000 psia independent of the time taken to accomplish the charge.

2.2 Engineering Prototype System Description

Although analysis of the system components other than the compressor and accumulators was not part of the scope of the charge rate study described herein, a brief description of the overall prototype system is included for completeness. A schematic of the system is shown in Figure 1.

In addition to the compressor and accumulators, the basic deliverable system consists of the following major components:

- Dryer
- Coolers
- Filters
- Instrumentation Transducers
- Electronic Drive and Controls
- Miscellaneous Block, Safety, and Check Valves

2.2.1 Dryer. Since moisture content of the inlet oxygen is greater than the allowable discharge moisture content, it is clear that some type of moisture removal component will be needed. Two common approaches to moisture removal are 1) condensation via a refrigeration loop (dehumidifier), and 2) absorption via a suitable desiccant (drying) agent. Since desiccant drying is a much simpler and less power-consumptive approach to moisture removal than is refrigeration condensation, a $CaSO_4$ desiccant dryer at the inlet to the HPOCS, with provision for easy removal and regeneration of the desiccant cartridge, is anticipated.

2.2.2 Coolers. To minimize temperature rise of the oxygen during the compression process, a two-stage compressor with intercooling between stages, as well as aftercooling of the final discharge gas will be employed. Because of the low flow rates involved, these will be small liquid-cooled heat exchangers. It is intended that the coolers can be integrated into the compressor structure, thus eliminating the need for external coolers.

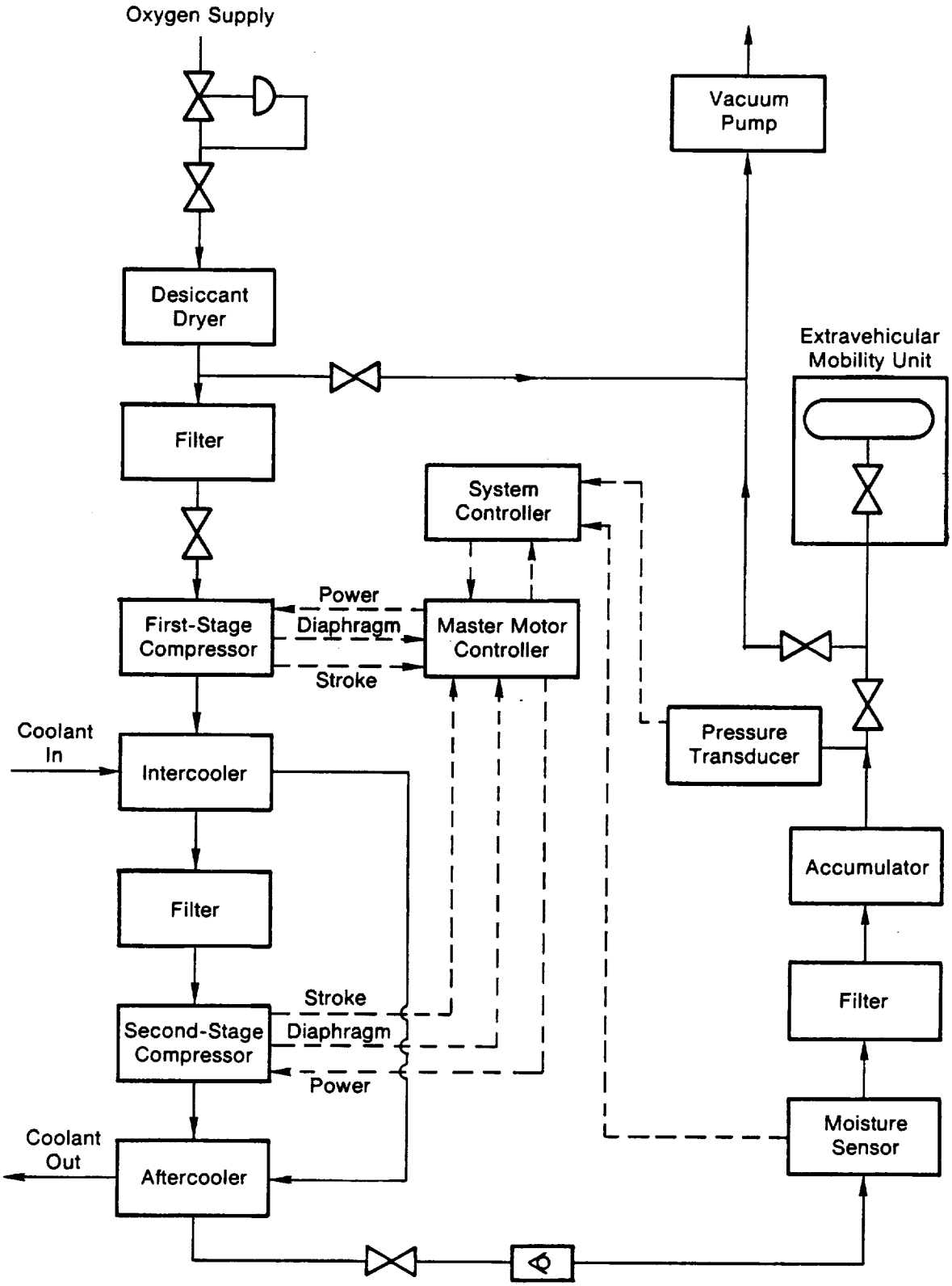

Figure 1 Preprototype Laboratory HPOCS

88075

2.2.3 Filters. Since high-velocity particles can be a source of ignition in high-pressure oxygen systems, it will be desirable to provide a filter at the inlet to the compressor, and possibly at the discharge, as well.

2.2.4 Instrumentation Transducers. The compressor concept will require specialized transducers to monitor dynamic operation of the compressor, in addition to pressure and temperature transducers to monitor and regulate system operation.

2.2.5 Electronic Drive and Control Circuits. Electronic circuitry will be required to power and control the linear reciprocating drive motors of the two-stage compressor. For the preprototype development, standard commercial electronics will, for the most part, be used. For the final space station HPOCS, development will be required to convert these electronics to space qualified packages. The control system is briefly discussed in Section 3.3.

3.0 COMPRESSOR DESIGN

3.1 Overall Compressor Description

The preliminary design of the HPOCS compressor is based on the concept of a two-stage diaphragm compressor hydraulically driven by linear motors. A drawing of the concept sized for a 6.0 lb/hr output is shown in Figure 2.

In each stage of the compressor, a thin metal diaphragm forms the movable boundary of the compression chamber. The back side of the diaphragm is in contact with water which fills the linear motor/hydraulic driver cavities. The diaphragm is actuated by the motion of a hydraulic piston that generates a pressure variation in the water-filled hydraulic cylinder. The piston, in turn, is driven by a linear motor mounted in the water-filled pressure vessel. In the design shown, the piston/motor stroke is approximately 0.85 in. The hydraulic piston/linear motor system is a resonant dynamic system, with a frequency of 25 Hz at 6000 psia discharge pressure for the compressor shown in Figure 2.

Plunger strokes of both the first- and second-stage compressors are maintained equal at all times and are always 180° out of phase. Magnetically excited stroke sensors are included to provide appropriate signals to the control system which maintains equal strokes. Since the masses of the two plunger assemblies are equal, the resulting equal and opposing strokes ensure that the fundamental component of vibration imposed on the compressor case is always zero. Due to the nonlinear characteristic of the compressors, higher harmonics of vibration will be present at some operating points, but this vibration will be very small.

The primary source of "springing" for the plungers is the effective spring rate of the compression process. Also, some spring effect is provided by the linear motors when the discharge pressure is less than 6000 psia. For the design shown, the effective spring rate from the compression process is 415 lb/in. at the high-pressure operating point. Thus the plunger mass has been selected at 6.5 lbm to achieve resonance at 25 Hz. As described later, the operating frequency is adjusted downward at discharge pressures less than 6000 psia. This allows near resonant behavior to be maintained for both stages over the entire

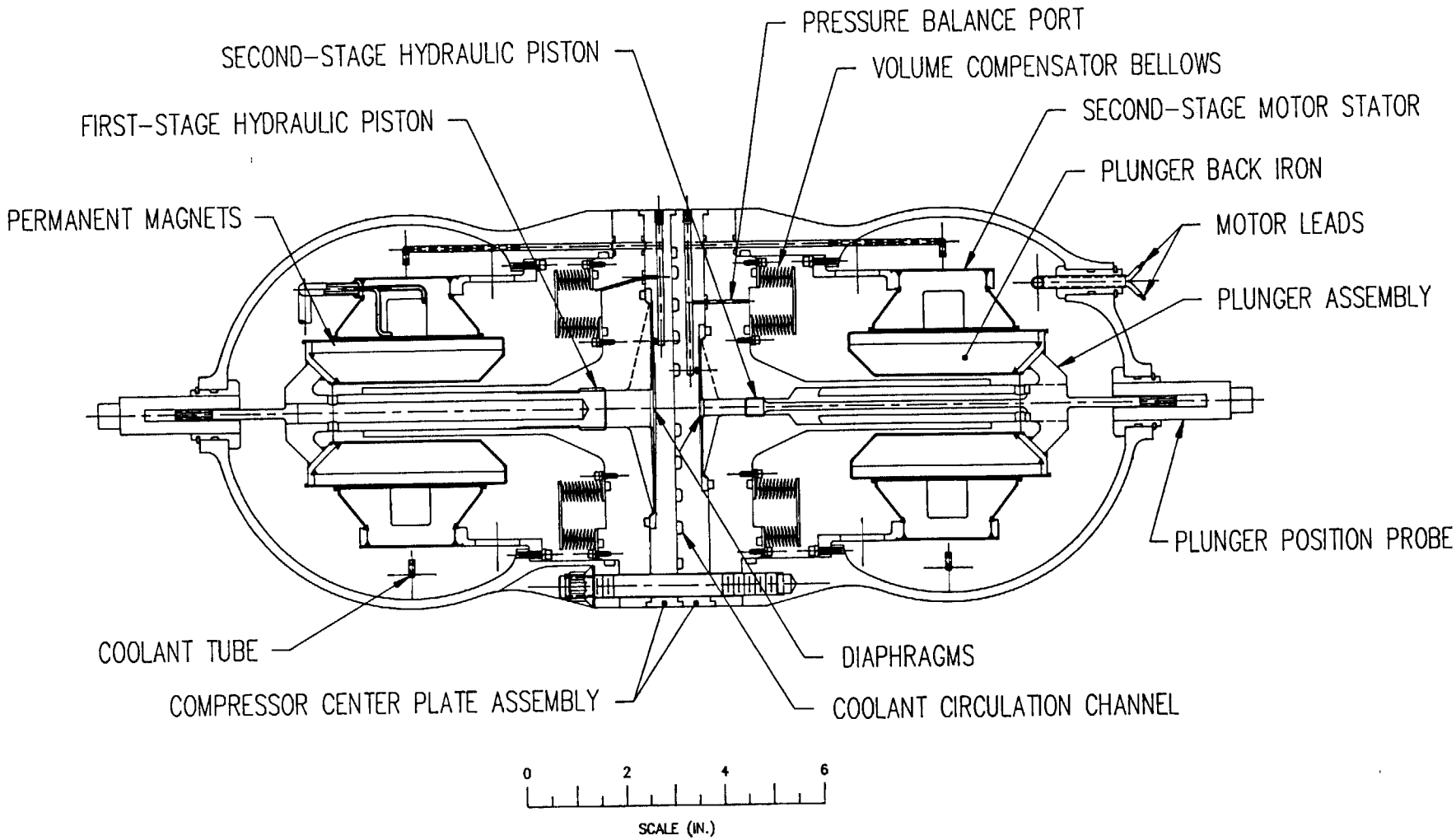

Figure 2 6.0 lbm/hr 25 Hz Oxygen Compressor

operating range. Mechanical centering springs are not needed because the linear motors provide strong magnetic centering for the plungers.

To accommodate changes in water volume due to thermal expansion and compressibility, and to allow for the water displaced by the piston motion, volume compensator bellows are incorporated within each of the motor cavities. These bellows are fabricated entirely from K500 Monel and are similar to commercially available components. The bellows are stressed to very low levels and should present no reliability or life-limiting problems. The magnitude of volume compensation required from the bellows is calculated from the thermal expansion coefficient of water, its compressibility, and the total volume of water displaced in each stage of the compressor.

The inside of each bellows assembly is pressurized with oxygen by means of a pressure balance tube connected to the compression chamber. A restrictive porous plug is installed in the top of each compression chamber to dampen the compression space pressure wave. Thus, the pressure balance tube is maintained at approximately the mean pressure in the compression space. Diaphragm centering depends on the exact match of water-side mean pressure and the mean pressure of oxygen in the compression chamber. The primary means of ensuring diaphragm centering will be achieved by center porting of the hydraulic pistons, coupled with active control of the motor/piston midstroke position.

The following is a brief summary of the salient features of the compressor design:

- Hermetic Isolation of Oxygen Flow Path

  The oxygen flow path through the compressor will be hermetically isolated from the compressor drive mechanism via the use of water-backed K500 Monel metallic diaphragms. The only materials in contact with the oxygen will be K500 Monel. There are no dynamic seals, hence no oxygen leakage, and no debris-generating sliding-contact or fretting surfaces within the oxygen environment.

- Entire Compressor Sealed within Pressure Vessel

  The entire compressor (including the water-flooded, linear-motor drive units) is sealed with a K500 Monel pressure vessel rated to contain HPOCS working pressure with a safety factor of three on ultimate strength.

- Long-Life, Canned, Linear-Motor Drive Units

  Each stage of the two-stage diaphragm compressor is driven by a brushless, reciprocating, permanent magnet, linear electric motor. Both the motor stator and plunger assemblies are "canned" with K500 Monel to minimize ignition potential in the event of a diaphragm failure.

  Motor power is hydraulically transmitted to the diaphragms using water as the hydraulic fluid. The water also serves as a lubricant for the drive bearings and hydraulic cylinder seal. This permits the bearing and seal surfaces to achieve very long wear life. Any wear debris from these surfaces will be hermetically isolated from the oxygen flow path.

- Low Vibration and Noise

  The two linear motors will be electronically controlled such that the reciprocating plunger masses are driven at the same frequency and stroke, but 180° out of phase. This provides excellent dynamic balance of the compressor assembly. As a consequence of the very low vibration levels, and the fact that the complete compressor assembly is sealed within a pressure vessel, compressor noise will be minimal.

3.2 Compressor Design Considerations

3.2.1 Diaphragms. The key elements in the proposed compressor design are the diaphragms. Contoured diaphragms are used as the positive displacement components in the compression chambers of the two-stage compressor. The contoured diaphragms are thin, flat, circular metallic plates capable of finite deflection without damage. The thickness of the contoured diaphragms varies with the radius in order to distribute the stresses as equally as possible over the face of the diaphragm. The thinnest region occurs about one-half the distance from the

center to the outer rim. Gradual thickening of the cross section occurs toward the hub and toward the outer rim.

For the purposes of this Task 1 effort, the criteria used to size the diaphragms was that the maximum radial bending stress was limited to 17,100 psi. This value represents the infinite fatigue life of K500 Monel with appropriate modifying factors for surface finish, stress concentration, 0.9999 reliability, and a 25% safety margin included.

As shown in Figure 2, the rim and central hub on the oxygen side of the diaphragms will be ground flat to facilitate shaping the compressor head for minimum clearance volume.

3.2.2 Linear Motors. The linear motors used to drive the compressors are stationary coil, moving-permanent-magnet motors using either samarium cobalt or neodymium-iron-boron magnets. The motors consist of two major components: a stationary outer stator and a moving inner plunger. The motors shown in Figure 2 are monocoil designs.

The outer stator is cylindrical and is made up of a multiplicity of identical flat laminations of a magnetically permeable material such as Hyperco 50. The laminations are oriented radially (in a manner similar to the cards in a Rolodex file) and are welded to forward and aft support rings to form a rigid structure. The laminations have a "U" shaped cross section with the open end of the U facing inward toward the motor centerline. As shown in the figure, the drive coil is nestled in the interior of the U.

The outer cylinder of the plunger is constructed of magnets and the inner cylinder is made of a magnetically permeable material. (The inner cylinder is called the backiron.) The backiron is also fabricated from a multiplicity of laminations that are taper-ground to achieve greater packing density. These laminations are oriented radially in a manner similar to that of the outer stator. The magnetic cylinder consists of a number of radially magnetized magnet segments bonded to the outer surface of the backiron. The magnets are arranged in three rings spaced axially along the plunger. The two outside rings are magnetized in one radial direction, and the single inner ring is magnetized in

the opposite direction. (The inner magnet is typically made longer than the corresponding outer magnets to compensate for coil opening.)

The outer stator and its coil, and the inner plunger and its magnets, are hermetically canned to prevent potential contact between the oxygen and the magnets or the coil potting compound if oxygen were to enter the motor area in the event of a diaphragm failure. Canning reduces the thickness of the magnet in the gap region and consequently reduces motor output. It also results in increased losses both directly (from the can eddy currents) and indirectly (as a result of the increased coil current required to make up for the loss in motor output). The inner canned plunger reciprocates concentrically within the outer canned stator. The physical clearance between the two structures is approximately 0.020 in.

- Linear Motor Losses

  By far the largest motor loss occurs in the stator plunger sheathing or cans (primarily in the gap region between these two structures). The sheathing loss is the result of circumferential eddy currents induced in the sheathing as the plunger reciprocates. At fixed stroke the sheathing loss is proportional to the frequency squared.

  The next most significant loss results from the I^2R drop in the main coil. This loss is primarily a function of the coil current squared and, consequently (since force is proportional to current), the motor force squared.

  Lesser losses are the result of stator and plunger hysteresis and eddy currents, magnet eddy currents, and eddy currents induced in the structures supporting the motor.

3.2.3 Diaphragm Centering. Controlling the position of the diaphragm in the proposed compressor system is an important design consideration. The diaphragm can be controlled using one of two methods:

- By allowing the diaphragm to lightly contact the head at the end of the compression stroke.

- By actively monitoring diaphragm position and varying the water volume behind the diaphragm to maintain centered operation without end-of-stroke contact.

The contacting approach is standard practice for controlling diaphragms in kinematic diaphragm compressors and is easily implemented as described in the following paragraph. The noncontacting approach has the advantage that there is no contact and, thus, no possibility for diaphragm wear and fretting. In addition it does not require additional bellows and check valve hardware.

- Contact Diaphragm Control

  Diaphragm displacement amplitude is closely tied to hydraulic piston motion, and the location of the diaphragm at any point in the cycle closely defines the motion of the diaphragm through the remainder of the cycle. End-stroke contact control takes advantage of this fact and allows absolute location of the diaphragm at the end of the compression stroke by coming into light, but solid, contact with the diaphragm head plate. To avoid excessive diaphragm stress and wear during contact, the overpressure associated with the contact is limited by a relief valve, and the head plate is contoured to conform to the shape of the diaphragm at maximum deflection.

- Noncontacting Diaphragm Control

  To actively control the center position of the diaphragm and prevent contact of the diaphragm with the head, the position of the diaphragm must be monitored, and the midstroke position of the motor adjusted. The key to this system is the design of the diaphragm position transducer. Ideally, the transducer for determining diaphragm location should be hermetically sealed, located on the water side of the diaphragm, able to accurately determine the diaphragm location over the full stroke, and be relatively insensitive to surrounding temperature, pressure, and stray

electric and magnetic fields. Although these requirements represent the ideal and are not all essential, it appears that they can be met by means of a mutual inductance probe or a fiber optic/digital probe and target system. Both of these types are currently being evaluated at MTI and the final choice between the two measurement approaches will be made based upon the results of this effort.

It is currently planned to pursue the noncontacting diaphragm control approach for the subject compressor because it avoids the potential for diaphragm fretting and thus, one potential source of failure or ignition.

Control of the water volume behind the diaphragm will be achieved by means of a port in the cylinder wall of the hydraulic piston coupled with a dc bias current in the drive motor. The motor dc bias current is used to vary the center position of the compressor piston and to change the timing of the port opening relative to the compression process. Moving the piston out results in the port opening when the water pressure in the compression chamber is high. This causes the water to flow out of the compression chamber and into the containment vessel and the diaphragm moves away from the head; that is, the clearance volume increases. Offset of the piston in the reverse direction results in an opposite diaphragm movement.

3.2.4 Compressor Valves. In any piston or diaphragm compressor, the suction and discharge valves are always critical components as regards both performance and life. For this application, there are two additional areas of concern, both related to ignition in a high-pressure oxygen environment. One is impact energy when the valve contacts its displacement-limiting stop during opening, or its seat upon closing. The second is generation of wear debris during the opening and closing impacts.

Two types of valves are normally used in positive displacement compressors. The most common type is the simple reed valve, which is designed using elastic beam theory for deflection, stress, and dynamic analysis. A less frequently used compressor valve is the poppet (ball check) type of valve. This type of valve is usually limited to low-flow, low-frequency applications. Because of the limited space (to minimize dead volume) available for valving, reed valves made of K500

Monel appear to be the most suitable choice for the subject application. Silver- or gold-plated seats will be considered to minimize flammability potential and increase valve life.

3.2.5 Bearings and Seals. Each linear-motor drive unit will require bearings for the motor plunger, and a clearance seal for the hydraulic piston. These bearings and seals will operate immersed in water. As a consequence of the light loadings imposed on these reciprocating parts, hydrodynamic (i.e., fluid film) lubrication should be obtained, with a resultant probability of very long component life. Nonetheless, it is highly desirable, if not mandatory, to select bearing and seal materials that are known to have low wear rates under wet sliding-contact conditions. This will ensure that these components will function well during compressor start-ups, as well as provide long life if the lubrication regime should be boundary layer, rather than hydrodynamic.

Ideally, the relative-motion surfaces of the bearings and piston seal should consist of a hard versus a soft wear couple combination. For example, a hardened metallic bearing journal running against a carbon-graphite sleeve would be an excellent choice under water-lubricated conditions. However, there is significant concern that carbon graphite would be subject to ignition if exposed to a water-oxygen mixture in the event of a diaphragm failure. Glass-filled PTFE sleeves, instead of carbon-graphite sleeves, would likewise be a very good choice for long-life, water-lubricated service. Phosphor bronze is yet another material combination which can be considered for the water-lubricated bearings and piston seal. Phosphor bronze is a common bearing material frequently used in water-lubricated pump bearings. Phosphor bronze is more acceptable from a flammability consideration in a water-oxygen environment than are the carbon-graphites or PTFE's. Accordingly, it is currently considered the preferred material for the bearing and seal sleeves.

Structural parts of the bearings and seal, such as the bearing shaft, piston rod, and piston, will be made of K500 Monel. Several techniques are available to provide hardened bearing and seal surfaces on the Monel. Hard nickel or chrome plating are conventional approaches; flame spraying of various oxide coatings, such as chrome oxide or aluminum oxide, is also a well established technique for obtaining high surface hardness. These various hardening tech-

niques will be evaluated for suitability to this application during the compressor design phase (Task 2.0) of this program.

3.2.6 Structural Analysis. The oxygen compressor system contains only a few structural components: the pressure vessel, flange bolts, motor stator mounts, and the piston carriers. Of these components, the pressure vessel and flange bolts are critical from a safety standpoint. K500 Monel was chosen as the material for the structural components. The combination of good strength, ignition resistance, and reasonable fatigue properties suggests it to be the prime choice. The flange bolts will be metric grade 12.9 alloy steel (minimum tensile strength 180 ksi).

The pressure vessel is sized based on three stress criteria. The first criterion specifies a minimum safety factor of 4.0 on the ultimate strength at the maximum normal operating pressure. The maximum mean operating pressure for the second stage is 3234 psia (including capillary pumping effects from the porous plug restrictor). The second criterion specifies a minimum safety factor of 1.5 on yield strength at 6000 psia. The vessel would only witness this pressure level if a check valve failure occurred and substantial quantities of high-pressure oxygen leaked back to the compressor. The third criterion specifies a 2.0 minimum safety factor guarding against fatigue, assuming 100,000 cycles from zero pressure to the maximum operating pressure. This criterion accounts for the pressure fluctuations in the vessel during its normal operating life.

The bolts are selected based on two criteria. Assuming a maximum internal pressure of 6000 psi, the bolts will exhibit a 1.5 safety factor against yielding. Also, the bolts will have a minimum safety factor of 2.0 against fatigue for 100,000 cycles. The loads on the motor stator mounts and piston carriers are relatively low, but go through complete reversals at the motor operating frequency. Therefore, these components will be designed to have a fatigue safety factor of at least 2.0 for an infinite number of cycles.

3.3 Control System Description

Although work on the HPOCS control system was not included in the Task 1.0 efforts, it is described herein for compeleteness. The HPOCS control system

controls the overall compressor system, which includes the two-stage compressor and linear motors, dehumidification equipment, and associated valving (see Figure 1). The primary functions of the HPOCS control system are to maintain required system performance; maintain safety of personnel and equipment; provide for reasonable evaluation of system performance (i.e., diagnostics); and provide a straightforward user interface. A two-tier system hierarchy, illustrated below, will be utilized to control these functions.

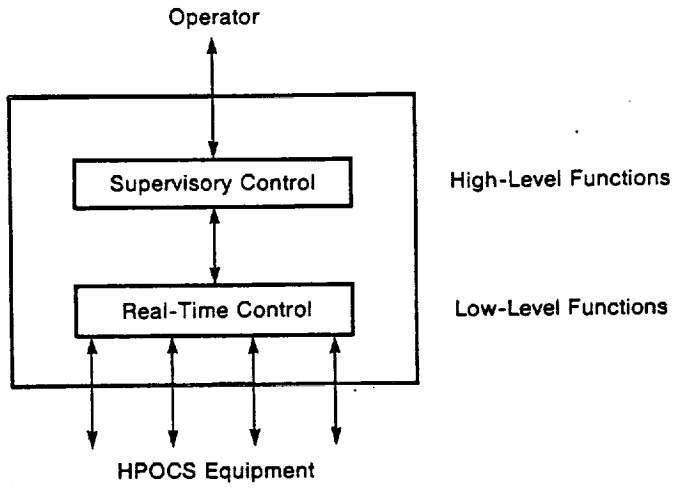

The HPOCS two-stage compressor is the primary component that will require real-time control. This function will consist of controlling the amplitude, phase, frequency, and mean value (dc offset) of the drive voltage provided to each of the linear motors. These motor control systems must satisfy four overall objectives, which include 1) maintaining the design stroke, 2) providing balanced first-harmonic operation, 3) ensuring proper operating frequency at operating pressure ratios less than 30.0, and 4) maintaining the mean level of the motor signal to control the mean diaphragm position. These functions and control methods are summarized in Figure 3.

The motor amplitude control will modulate the voltage amplitude of the drive motor signal to maintain fixed and equal strokes of the motor/piston. This stroke, which in turn determines the diaphragm deflections and flow capacity of the compressor, is thus fixed.

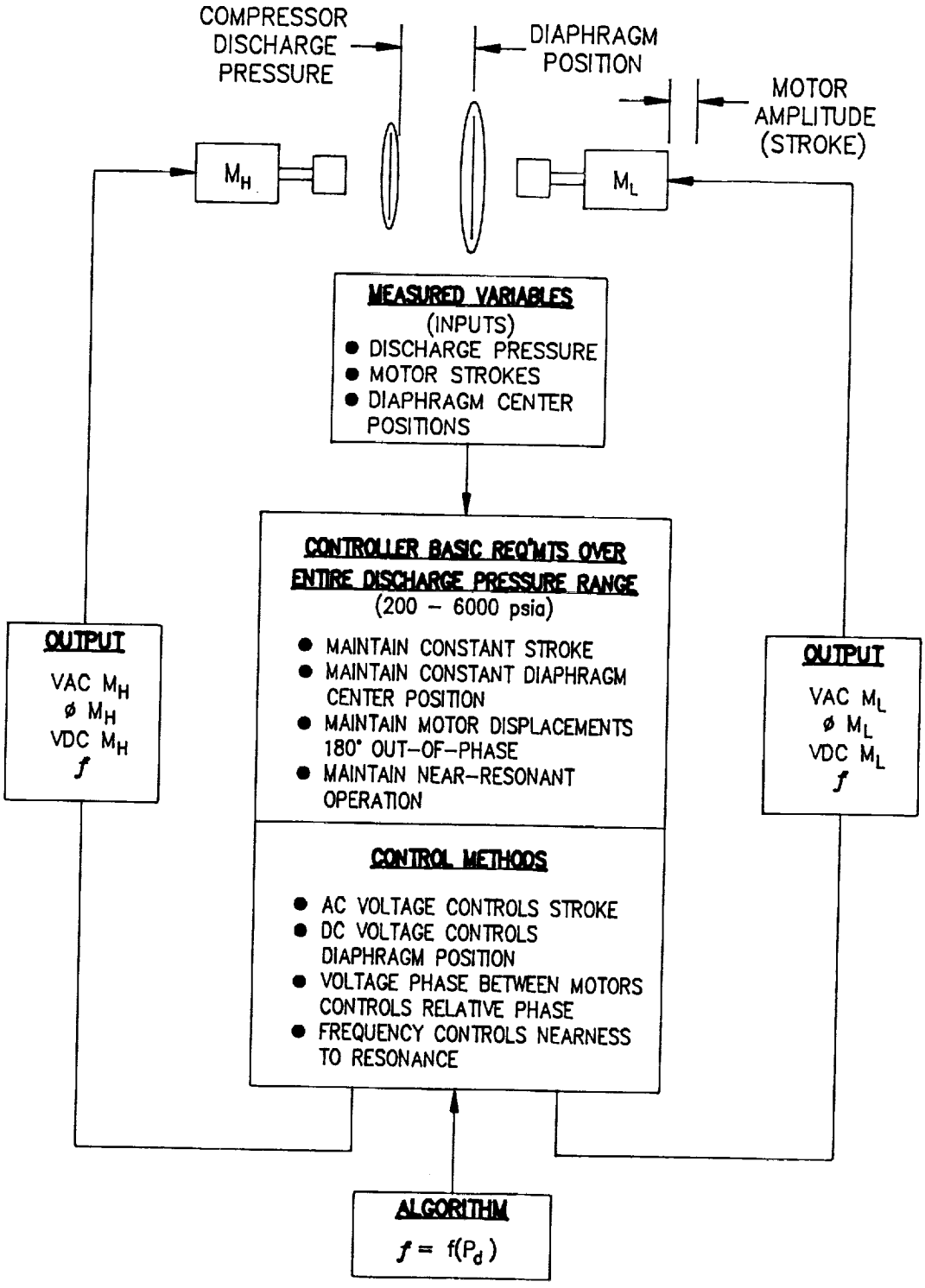

Figure 3 Summary of Control System Functions

The phasing of the two motors will be maintained 180° out of phase, such that the first harmonic of the motor forces will be equal and opposite, thus resulting in the dynamic balancing of the unit. The frequency of the two drive voltage signals will also be identical, although the value of the frequency will be controlled to maintain a constant "tuning offset" of each stage. This control would not be required if the compressor operated at a constant pressure ratio; however, since the compressor pressure ratio will vary between approximately 1.0 and 30.0 as the tanks are filled, the resonant frequency of the first and second stages will not be equal at pressure ratios less than 30.0. The frequency control will maintain the drive frequency at a value between the individual stage resonant frequencies. This will result in a matched "tuning offset" between the drive voltage frequency and the resonant frequency of the individual stages at intermediate pressure ratios. The control of the mean value of the drive voltage (dc offset) will control the midstroke position of the hydraulic piston, thus controlling the mean position of the diaphragm. The four real-time control requirements will be met through the use of feedback control loops based on motor position and diaphragm position sensor inputs.

The motors will be driven by independent power amplifiers which will allow control of the amplitude and dc offset of the periodic signal. The amplifiers will be driven by a variable-frequency signal generator to maintain identical frequency inputs. The periodic signals provided by the signal generator may be either square wave or sinusoidal wave forms.

It is desirable to use square wave signals from the standpoint of overall electronics simplicity. (The ability to operate in the presence of the harmonics introduced by square wave drives will be determined during preprototype evaluation.) The drive signal will be amplified to the power levels (current and voltage) required by the linear motors.

The supervisory control functions provide the high-level coordination of real-time control necessary to meet performance, safety, and operational requirements. There are four major functions associated with the supervisory control systems; these are sequential control, safety, diagnostics, and user interface.

Sequential control functions provide the necessary control logic (sequencing) required for fully automatic start-up, shutdown, and normal running of the HPOCS.

The start-up sequence is initiated in response to recognition of an operator requested "cycle start." A typical start-up sequence would be as follows:

1. Check bottles connected to system (contact closure)

2. Check HPOCS connection to oxygen source (is 200-psi supply pressure present?)

3. Close compressor discharge return bleed valve

4. Open compressor discharge shutoff valve

5. Open inlet shutoff valve

6. Start compressor (soft start via ramping of linear motor drive signal amplitudes to required control values)

The shutdown sequence is initiated in response to completion of the charging cycle or a detected system fault. A typical shutdown sequence is:

1. Ramp compressor stroke amplitude to zero

2. Close compressor discharge shutoff valve

3. Close inlet shutoff valve

4. Open compressor discharge return bleed valve

5. Indicate charge cycle complete

The supervisory control safety functions monitor HPOCS operating conditions to identify system anomalies affecting equipment and personnel safety, and initi-

ate appropriate action in response to detected anomalies. Safety-related faults result in shutdown of the HPOCS system and an indication of the detected fault condition(s). Safety faults that may be detected include, but are not limited to, high vibration levels, high oxygen humidity levels, low charge rate (trip level), linear motor power supply fault (overcurrent), and sequence fault (no bottle and/or source oxygen detected at start-up).

The supervisory control also governs diagnostic functions which include, but are not limited to, an indication of a low charge rate (alarm level) or that a desiccant change is required.

The supervisory control user interface is the means by which the operator controls and monitors operation of the HPOCS. The user interface includes a dedicated operator's panel containing various indicators, switches, and buttons, i.e., cycle start button to initiate the charge cycle; an emergency stop button; gages for Stage 1 discharge pressure, Stage 2 discharge pressure, and supply pressure; and LED's to indicate safety or diagnostic faults, and to show that the cycle is complete.

4.0 PERFORMANCE ANALYSIS

Figure 4 outlines the analysis procedure employed during the conduct of the HPOCS charge rate study. The upper line of blocks indicates those tasks that are required to size the compressor/motor assemblies to achieve the design point discharge pressure of 6000 psia (with an inlet pressure of 200 psia) for the various design flow rates considered. For the purpose of this study, the following design flow rates (at 6000 psia discharge) were considered: 0.75, 6.0, and 11.82 lb/hr.

The middle line of blocks outlines those tasks required to determine the compressor performance at off-design conditions, i.e., over the range from 200 to 6000 psia discharge (the conditions encountered during actual tank charging, and the time and energy consumed during the tank charging process for various charging scenarios).

The lower line indicates the tasks required to determine compressor size and weight, and the final establishment of launch and energy costs.

The bin analysis of performance over a charging cycle and determination of launch and energy costs are discussed in Section 5.0 of this report. The actual compressor performance aspects are discussed in the following subsections.

4.1 Compressor/Motor Design Point Sizing and Off-Design Performance

The principal design parameters for the compressor are chosen primarily on the basis of dynamics. The basic premise being that resonant, or near resonant, oscillation of the plunger be maintained (resonant operation eliminates the need for the motor to provide plunger acceleration forces). Minimization of motor force leads to minimization of motor size and weight.

The parameter selection, based upon resonant free-piston dynamics, proceeds as follows. A volume amplitude is selected based upon the design flow rate and a frequency selection that results in a diaphragm geometry that meets the following constraints:

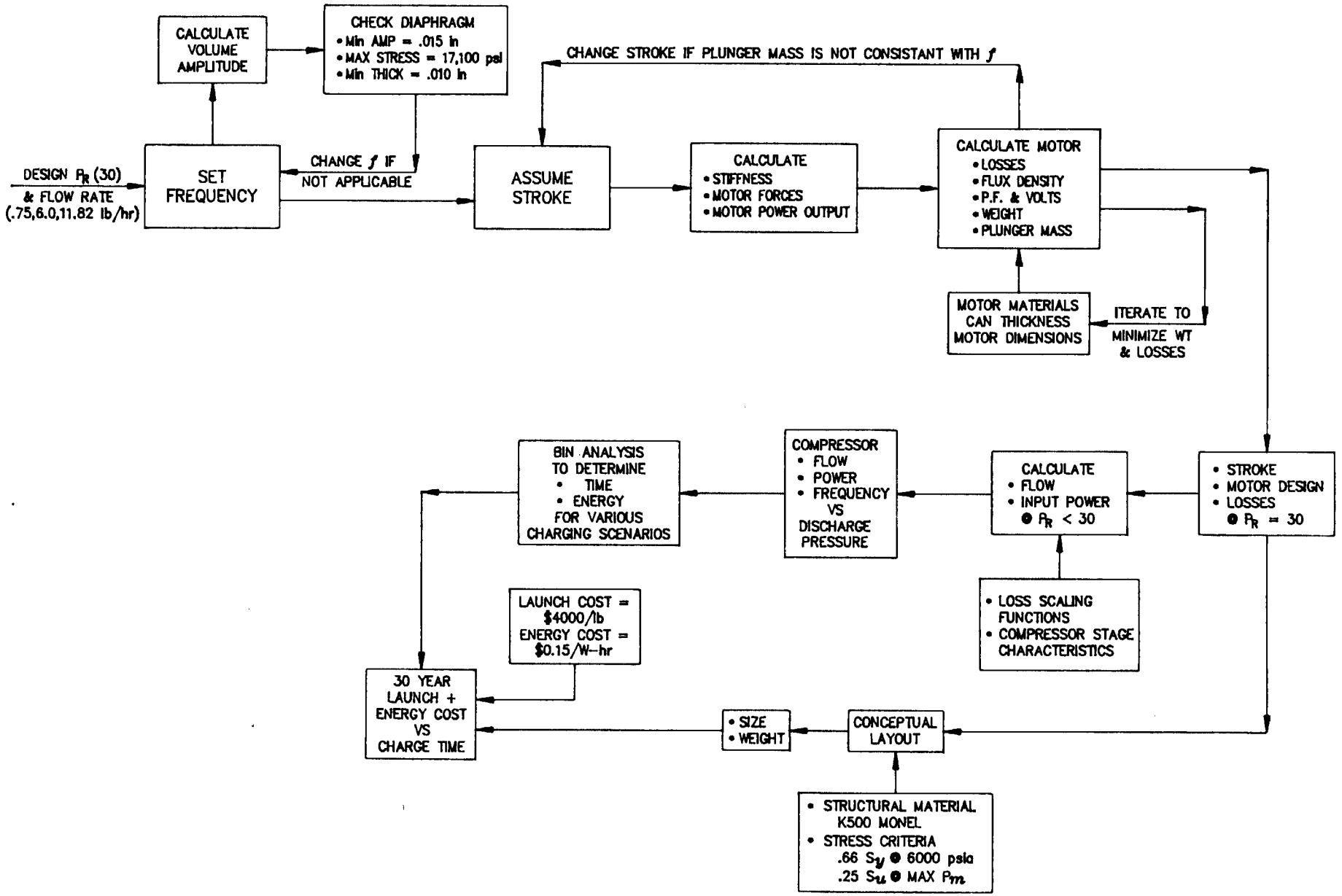

Figure 4 Outline of Charge Rate Study Analysis Procedure

- Minimum diaphragm amplitude must exceed 0.015 inches. This value was set based upon experience and judgement considering the practical aspects of minimizing compressor clearance volume and sensing diaphragm mid-stroke position.

- The maximum radial bending stress was set at 17,100/psi as discussed in Section 3.1.

- The minimum diaphragm thickness was set at 0.010 inches based upon previous successful manufacturing and operating experience.

A motor plunger stroke is then selected based upon motor sizing judgements. Next the compressor equivalent stiffness and required motor force and power is established based upon the compressor design point conditions (flow at 6000 psia), selected frequency, and stroke. These parameters set the requirements for the motor design.

The motor design is an iterative process where motor geometry is varied to minimize losses and weight. Motor materials (Hyperco 50 laminations, copper wire, samarium cobalt magnets, and 0.020 inch thick K500 Monel cans) were held constant for this study. Upon obtaining an acceptable motor design from a loss and size standpoint, the resulting plunger mass was compared with that required to achieve resonance at the initial selected frequency. If the mass was not within 10% of that required, a new stroke was assumed and the preceding process repeated. Also, during the motor design process, motor performance was checked at two compressor pressure ratios lower than 30.0 to make sure that its off-design performance would be acceptable.

Upon completing the preceding process, the following information was now in hand:

- Compressor diaphragm sizes (first and second stage)
- Motor plunger stroke and piston areas
- Motor geometry and weight
- Motor losses at a pressure ratio of 30

This information now permitted the design layouts and off-design performance of each compressor to proceed.

4.2 Off-Design Performance

Performance characteristics and layout designs were completed for four different compressors:

11.82 lb/hr with design point resonance at 25 Hz
6.0 lb/hr with design point resonance at 25 Hz
6.0 lb/hr with design point resonance at 32 Hz
0.75 lb/hr operating at a constant frequency of 5 Hz

Table I summarizes the operating characteristics of the 11.82 lb/hr compressor at pressure ratios between 1.0 and 30.0.

Predicted mass flow rates for the compressors were established using the basic isentropic analysis described in numerous textbooks covering positive displacement compressors. Clearance volume ratio is assumed constant at 0.30. Heat transfer plays a very important role in the final analysis of compressor performance. However, the performance predictions presented here do not include the effects of heat transfer during the compression process, thus adiabatic compression with intercooling to 70°F is assumed.

The machines were sized to achieve equal first- and second-stage pressure ratios when the total pressure ratio is 30, which corresponds to 6000 psia discharge pressure. At discharge pressures less than 6000 psia, the pressure ratio split between the two stages is unequal because the oxygen mass flow rate is the same for both stages and the strokes and clearance volumes are assumed to remain unchanged. A simple iterative procedure was performed on the computer to determine the pressure ratio split at each operating point listed on the table. Fourier analysis of the ideal compression cycle was then performed to find the mean pressure and effective spring rate.

For the 6.0 and 11.82 lb/hr machines, the frequency was controlled to a value equal to the average resonant frequency of the two stages. Lower frequency

Table I

11.82 lb/hr Compressor Performance at Various Pressure Ratios

Pr_{total}	f (Hz)	$\dot{m}$ (lb/hr)	Pr_1	Pr_2	Compressor Spring Rate (lb/in) K_1	K_2	Motor Shaft Power (watt) P_1	P_2	Motor Efficiency η_1	η_2	Active Motor Force (lb) FA_1	FA_2	Reactive Motor Force (lb) FR_1	FR_2	D.C. Motor Force (lb) F_{DC1}	F_{DC2}
30	25	11.82	5.477	5.477	584.13	584.13	361.38	361.38	.7156	.7156	81.44	81.44	0.0	0.0	68.9	68.9
26	23.72	12.79	5.172	5.027	549.12	502.47	367.7	360.71	.7329	.7347	87.34	85.68	-11.67	11.67	64.2	61.9
22	22.31	13.55	4.864	4.523	512.58	417.85	365.78	347.49	.7415	.7451	92.38	87.76	-23.68	23.68	59.4	54.2
18	20.74	14.05	4.551	3.955	474.04	329.92	355.03	319.26	.7444	.7501	96.45	86.74	-36.03	36.03	54.6	45.4
14	18.96	14.23	4.231	3.309	433.27	238.33	334.49	273.07	.7411	.7473	99.40	81.15	-48.74	48.74	49.7	35.5
10	16.89	13.99	3.900	2.564	389.65	143.38	302.88	204.77	.7301	.7291	101.04	68.31	-61.57	61.57	44.6	24.1
6	15.0	13.70	3.547	1.692	341.68	48.41	269.55	111.53	.7221	.6331	101.25	41.89	-65.70	80.94	39.2	10.6
2	15.0	19.81	2.0	1.0	118.71	0	200.7	18	.7598	.1917	75.39	6.76	45.79	105.37	15.4	0
1	15.0	24.52	1.0	1.0	0	0	18	18	.1917	.1917	6.76	6.76	105.37	105.37	0	0

limits of 15 and 18 Hz were set for the 25 and 32 Hz machines, respectively. At these frequencies, the reactive motor forces were small and further reduction of operating frequencies (at the lower pressure ratios) was deemed unwarranted.

In the case of the 0.75 lb/hr machine, the frequency was held constant at 5 Hz over the entire operating range. It should also be noted that this machine operates well below resonance under all operating conditions. The reason for this is that the low mass flow rate dictated an operating frequency of about 5 Hz or less to stay within the aforementioned diaphragm deflection constraint. Designing for resonant operation at 5 Hz resulted in a very long motor stroke and therefore resulted in excessive motor size and weight. By choosing a shorter stroke and nonresonant operation, a more reasonable motor size resulted, with total motor forces (reactive and active) not significantly different from the higher flow resonant designs.

The motor power requirements, P_1 and P_2 in Table I, were obtained by dividing the calculated adiabatic compression power by 0.8 and then adding the hydraulic loss. (Measured isentropic compressor efficiencies at MTI have typically been somewhat greater than 80%). The table also lists the active, i.e., power producing, and reactive, i.e., spring producing, motor force requirements for each pressure ratio. The hydraulic and motor losses were evaluated in detail at the design point (Pr = 30). The hydraulic loss and motor efficiencies indicated in Table I at pressure ratios less than 30 were derived from the following scaling rules:

- Hydraulic loss scales with (frequency x stroke)^2
- Motor lamination hysteresis scales with (frequency)
- Motor lamination eddy current loss scales with (frequency)^2
- Can eddy current loss scales with (frequency)^2
- Copper I^2R loss scales as a function of (total motor force)
- Magnet eddy current loss was neglected (<10 watts in all cases)

Figures 5 through 12 are plots of the mass flow rate and motor input power for each of the four compressor designs considered during this study. The way in which these curves were used in performing the actual charge rate study is described in Section 5.0.

4.3 Summary of Compressor Sizing Study

The significant parameters relating to each of the four compressor designs are summarized in Table II. The dimensions and weights shown were derived from actual preliminary layout drawings made for each compressor. The drawing shown in Figure 2 is typical of these layouts. "Total filled weight" includes the weight of the water in the motor cavity.

From Table II, it is seen that larger diaphragm amplitudes are attainable with the higher flow rate machines, and that for the same size machine (6.0 lb/hr), the lower frequency case produces the larger amplitude. Also shown in Table II are the times to pump 11.82 lb or oxygen (quantity carried in two EMU's at 6000 psia) from 200 psia to 6000 psia and the peak power consumption (at 6000 psia discharge pressure).

Figure 13 shows the compressor weights as a function of design flow. Although it is not possible to accurately define the shape of such a curve with the few (4) points actually calculated, it appears that the minimum weight compressor will be somewhere near a 4 lb/hr design.

Table III summarizes the general diaphragm compressor sizing trends and gives qualitative trade-offs with respect to selection of operating frequency.

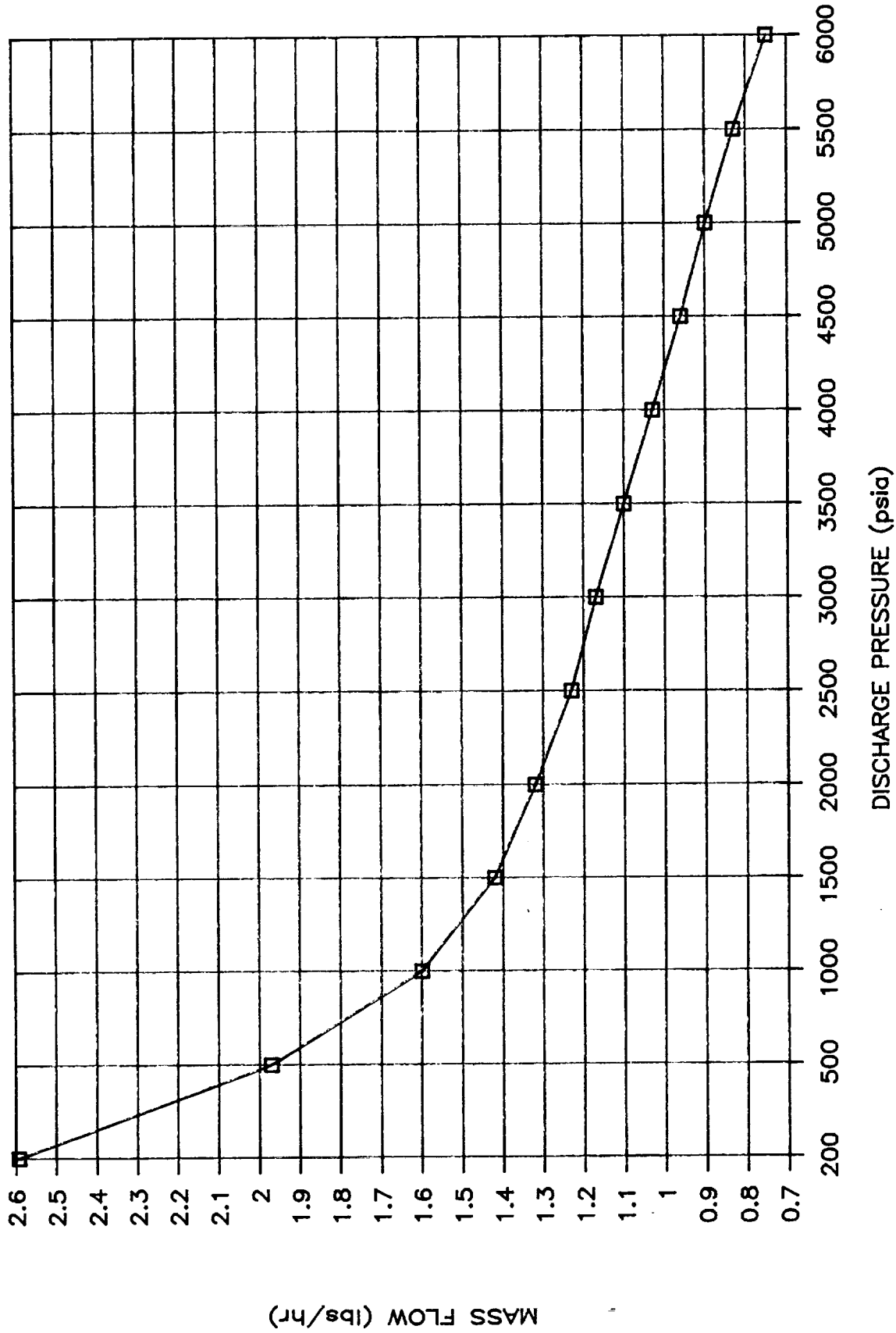

Figure 5 Flow vs. Pressure for 0.75 lb/hr, 5 Hz Compressor

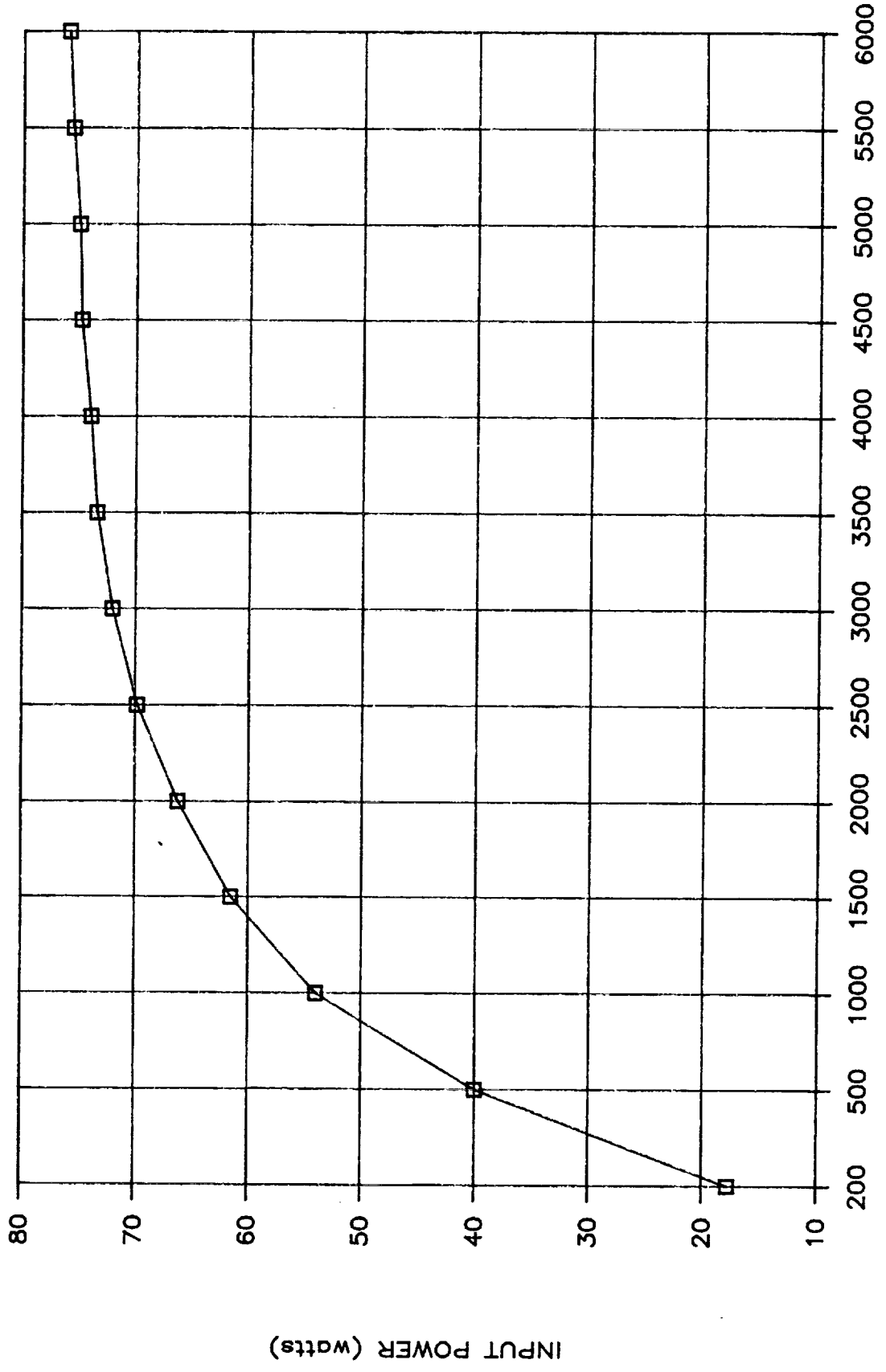

Figure 6 Power vs. Pressure for 0.75 lb/hr, 5 Hz Compressor

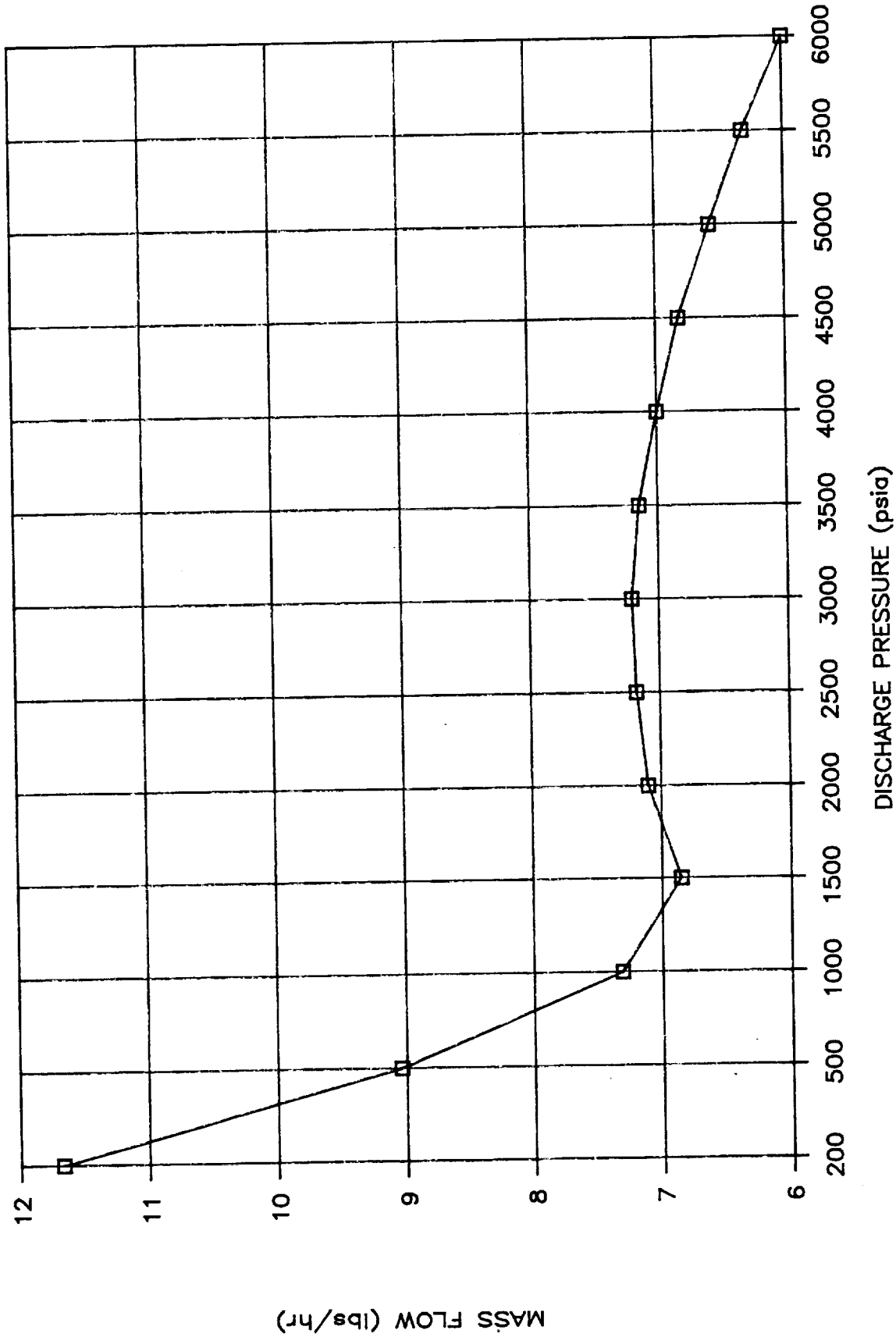

Figure 7 Flow vs. Pressure for 6.0 lb/hr, 32 Hz Compressor

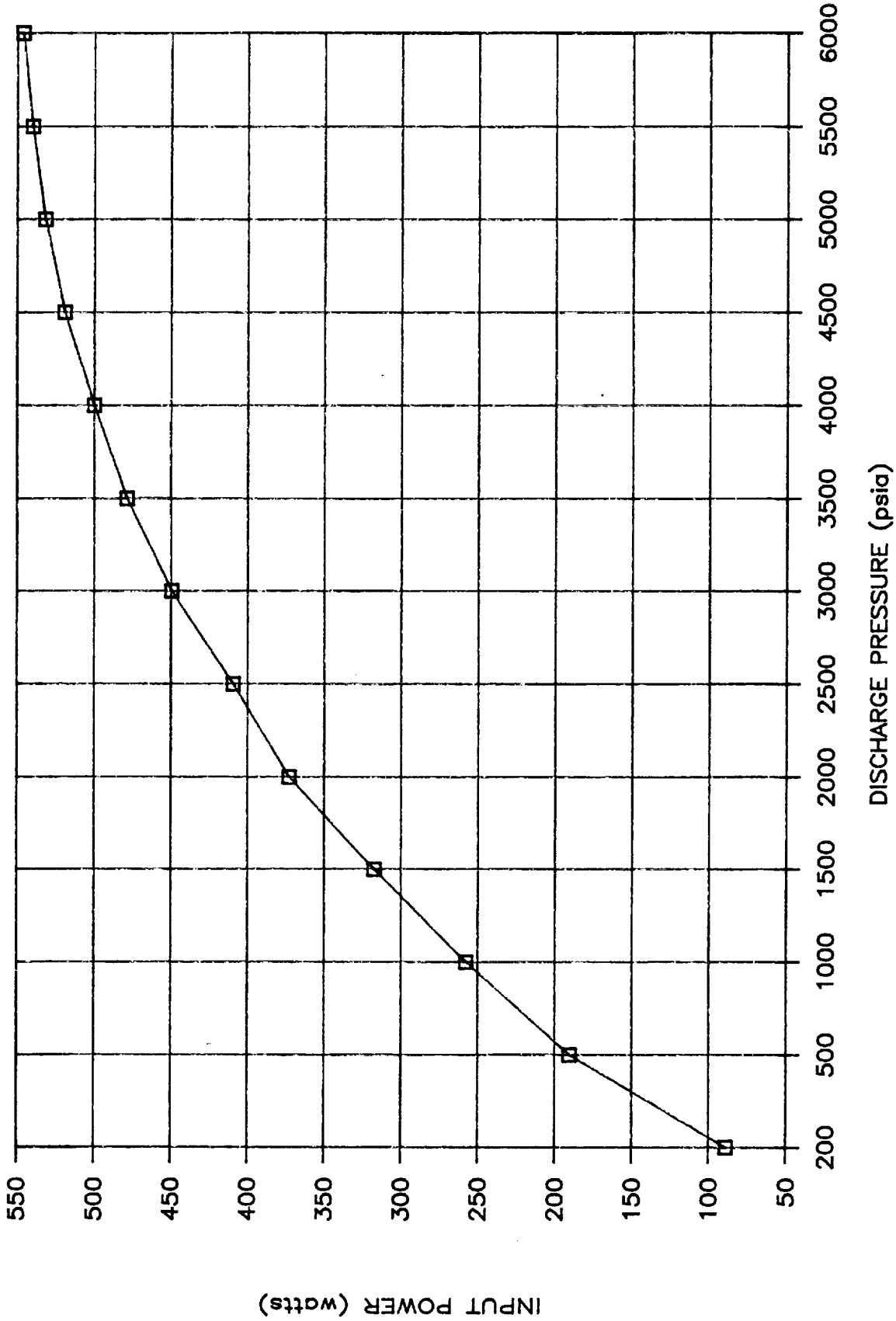

Figure 8 Power vs. Pressure for 6.0 lb/hr, 32 Hz Compressor

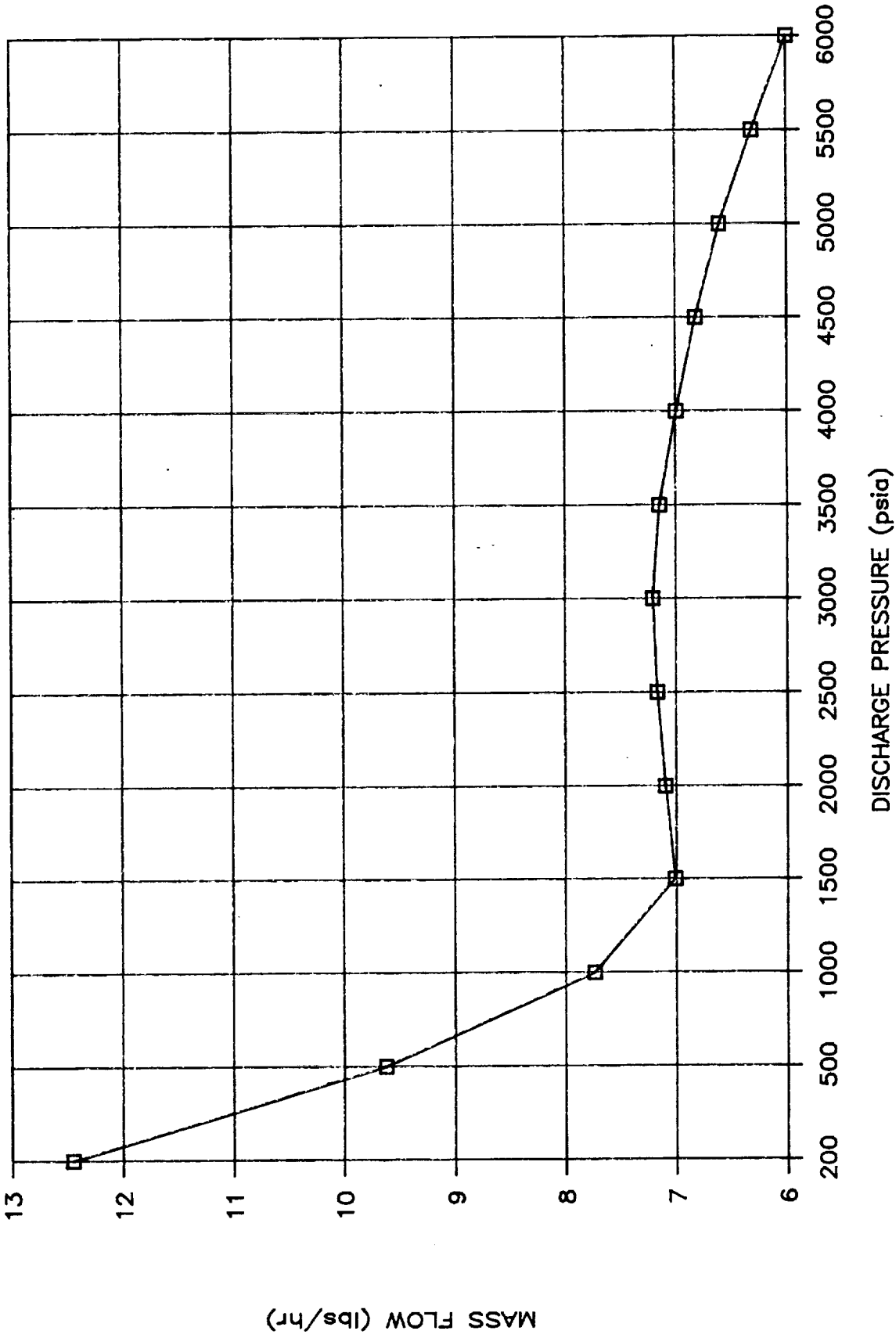

Figure 9 Flow vs. Pressure for 6.0 lb/hr, 25 Hz Compressor

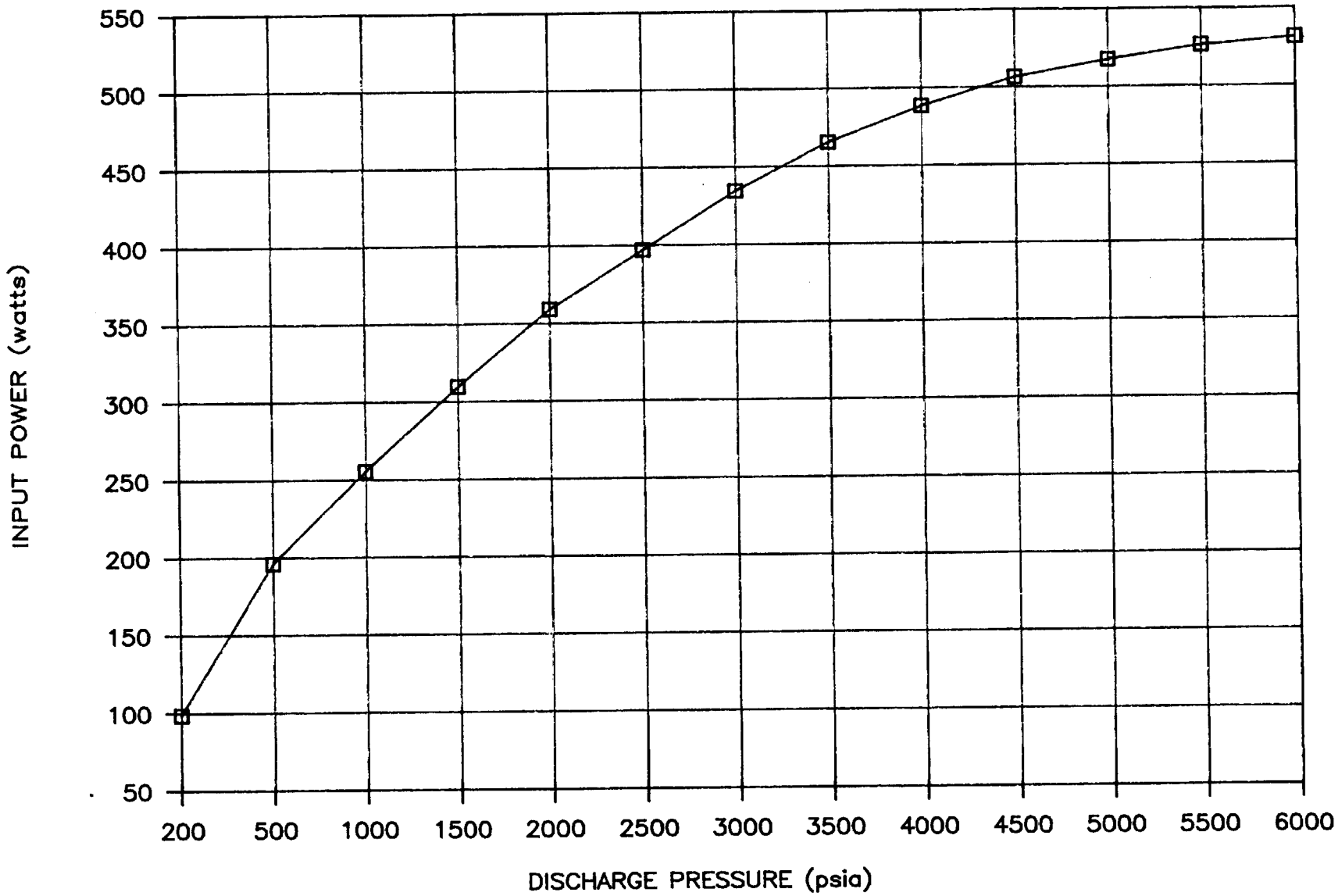

Figure 10 Power vs. Pressure for 6.0 lb/hr, 25 Hz Compressor

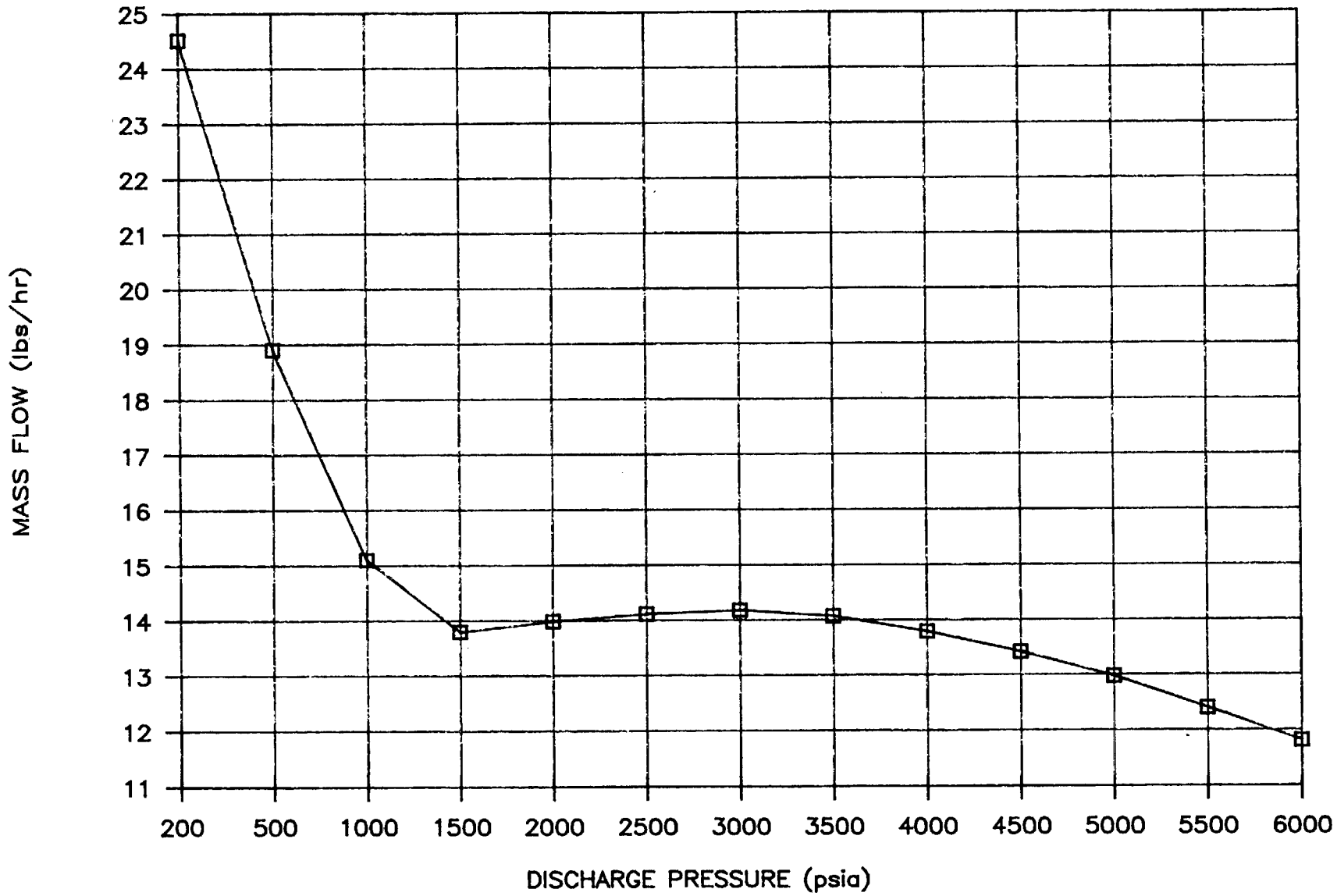

Figure 11 Flow vs. Pressure for 11.82 lb/hr, 25 Hz Compressor

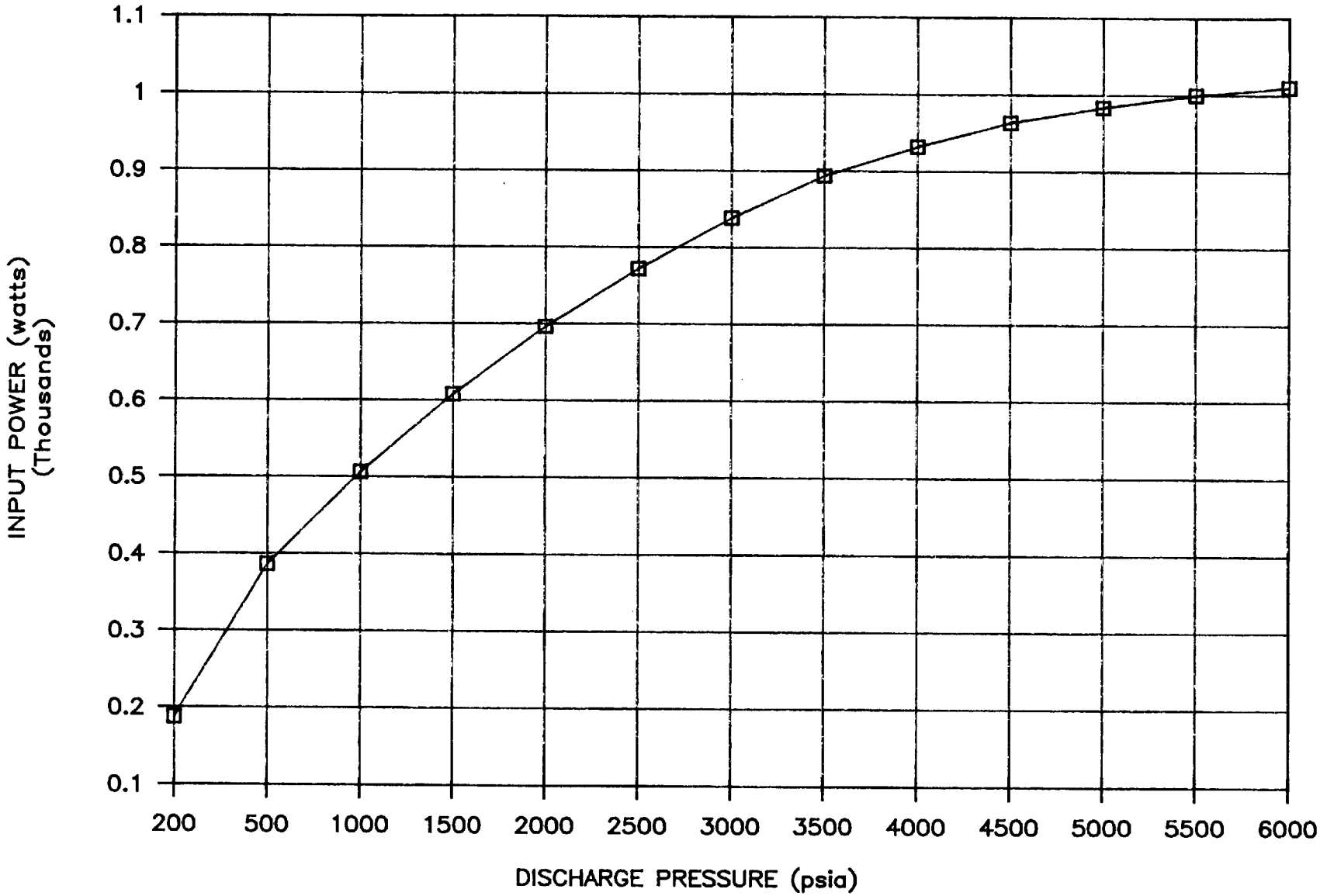

Figure 12 Power vs. Pressure for 11.82 lb/hr, 25 Hz Compressor

HPOCS - Summary of Significant Parameters by Mass Pumping

PARAMETER	MACHINE 0.75 lb/hr 5 Hz	6.0 lb/hr 25 Hz	6.0 lb/hr 32 Hz	12.0 lb/hr 25 Hz
TOTAL DRY WEIGHT	206.1	114.7	92.5	148.8
TOTAL FILLED WEIGHT	225.7 lbs	127.4 lbs	103.2 lbs	162.3 lbs
DIAMETER	10.6 in	7.9 in	7.3 in	8.9 in
LENGTH	22.4 in.	19.6 in.	18.3 in.	19.6 in.
OCCUPIED VOLUME	1977 cu.in.	961 cu.in.	766 cu.in.	1219 cu.in.
DIAPHRAGM AMPLITUDE (2ND STAGE)	.015 in.	.017 in.	.016 in.	.022 in.
TIME TO PUMP 11.82 lb.	10.2 hr.	1.59 hr.	1.61 hr.	0.81 hr.
ENERGY CONSUMED	692 W–hr.	665 W–hr.	687 W–hr.	650 W–hr.
PEAK POWER	76 WATTS	531 WATTS	546 WATTS	1010 WATTS

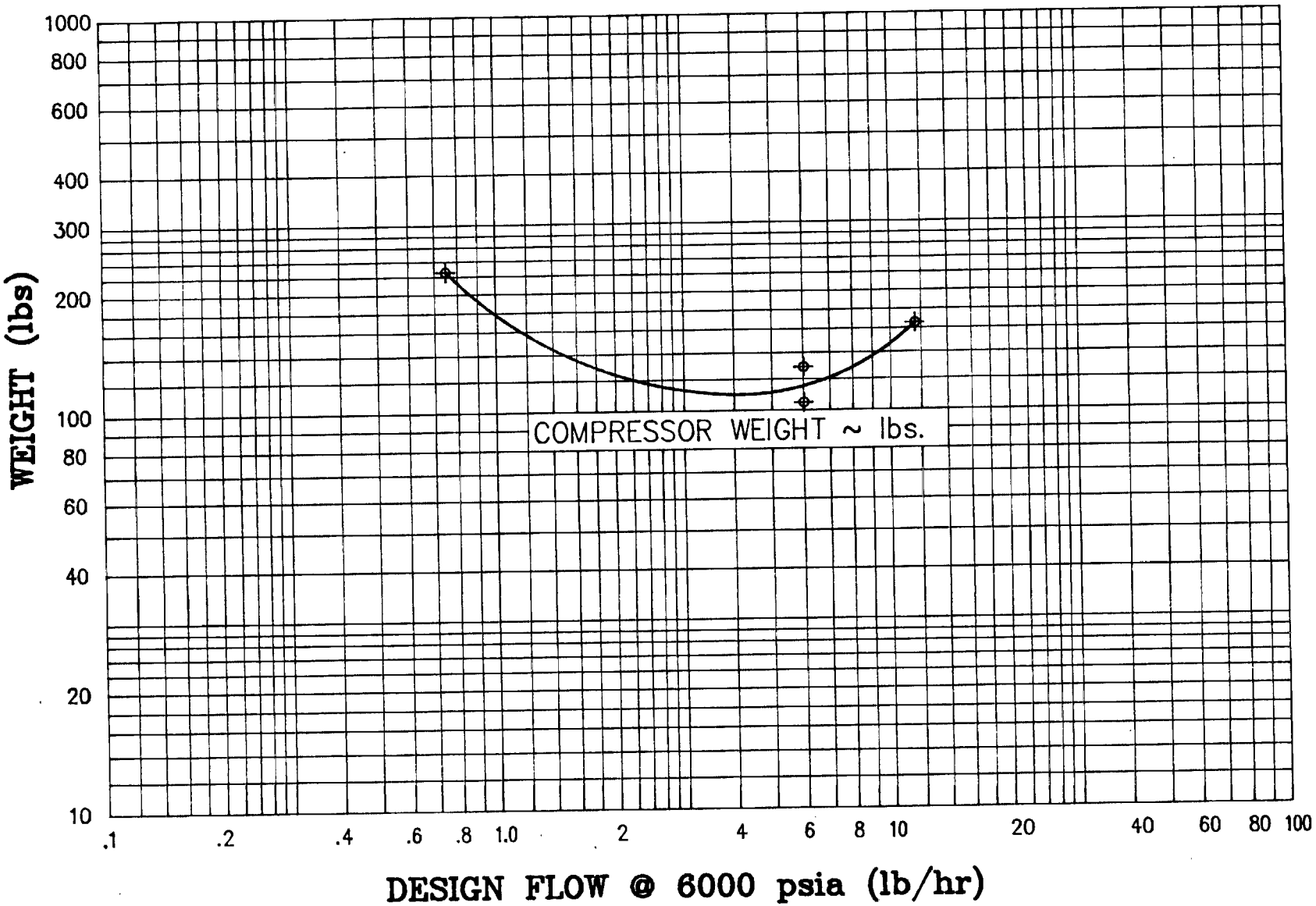

Figure 13 Effect of Design Flow on Weight

Table III

GENERAL COMPRESSOR SIZING TRENDS

- Maximizing frequency tends to minimize motor size and weight.
- The maximum frequency for any given design flow rate is set by diaphragm minimum amplitude and maximum stress constraints.
- The lower the flow rate the lower the maximum operating frequency.
- Higher flow rate (higher frequency) compressors tend to be lighter if run near resonance because the resulting smaller required motor forces lead to smaller motor size.
- Lower flow rate compressors tend to be lighter if run off-resonance because the high plunger stroke required to achieve resonant operation leads to large motor size
- For a given compressor flow rate, lower frequency tends to reduce losses.
- For a given flow rate the selected operating frequency is primarily a trade-off between diaphragm constraints, weight, and total energy consumption.

5.0 CHARGING SCENARIOS

Two basic PLSS charging options were considered; the direct charge and the accumulator charge. These are shown schematically in Figure 14. For the direct charge option, each PLSS consisting of two tanks is charged directly by the compressor. For the accumulator charge option, the compressor first charges an accumulator to 6000 psia and this precharged accumulator is then used to partially fill each PLSS. Then the accumulator is bypassed and the PLSS is fully charged (topped off) with the compressor. For the purpose of this study, three different accumulator sizes (volumes) were assumed: 0.1751, 0.3501, and 0.8755 ft^3. For the discussions that follow, the zero volume accumulator is equivalent to the direct charge use. The analyses presented in this section were performed assuming isentropic compressor behavior and isothermal accumulator/tank behavior.

Figure 15 depicts the assumptions made with regard to the normal oxygen usage for a typical EVA mission. These were as follows:

1. An EVA always involves two astronauts.

2. The total amount of oxygen carried by the two astronauts at the beginning of the EVA is 11.82 lbs (carried in a total of four tanks).

3. The initial charge temperature and pressure are 70°F and 6000 psia respectively.

4. The astronaut uses oxygen out of only one tank. The other tank is for emergency purposes only.

5. The normal mission usage is 1.478 lb per astronaut (2.955 lbs total) or one half the total inventory of two tanks.

These assumptions were based upon discussions and usage scenario data provided by NASA-JSC engineers.

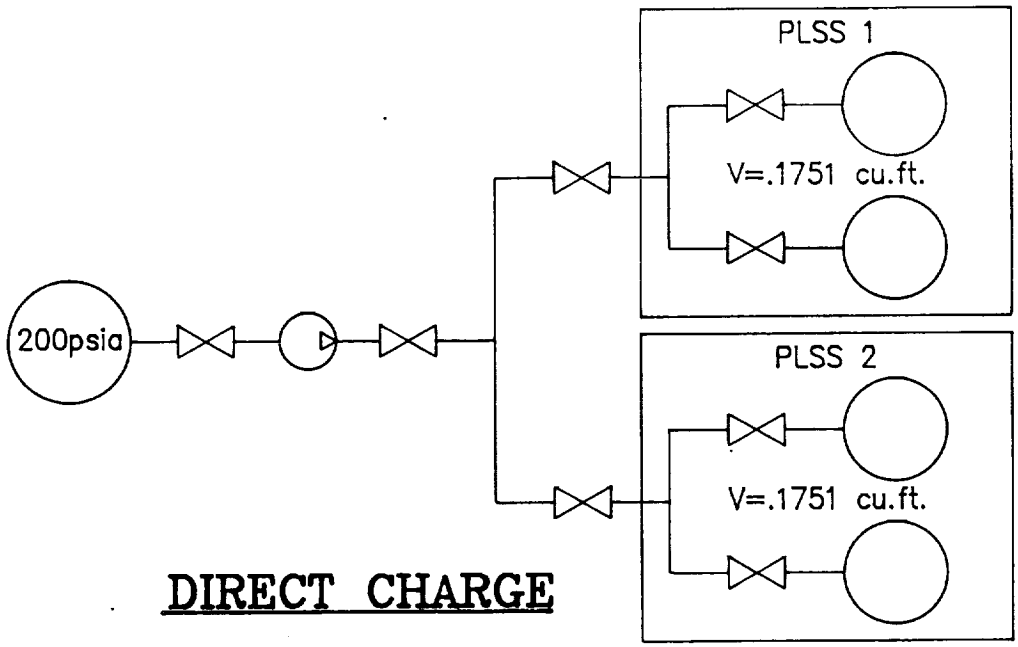

DIRECT CHARGE

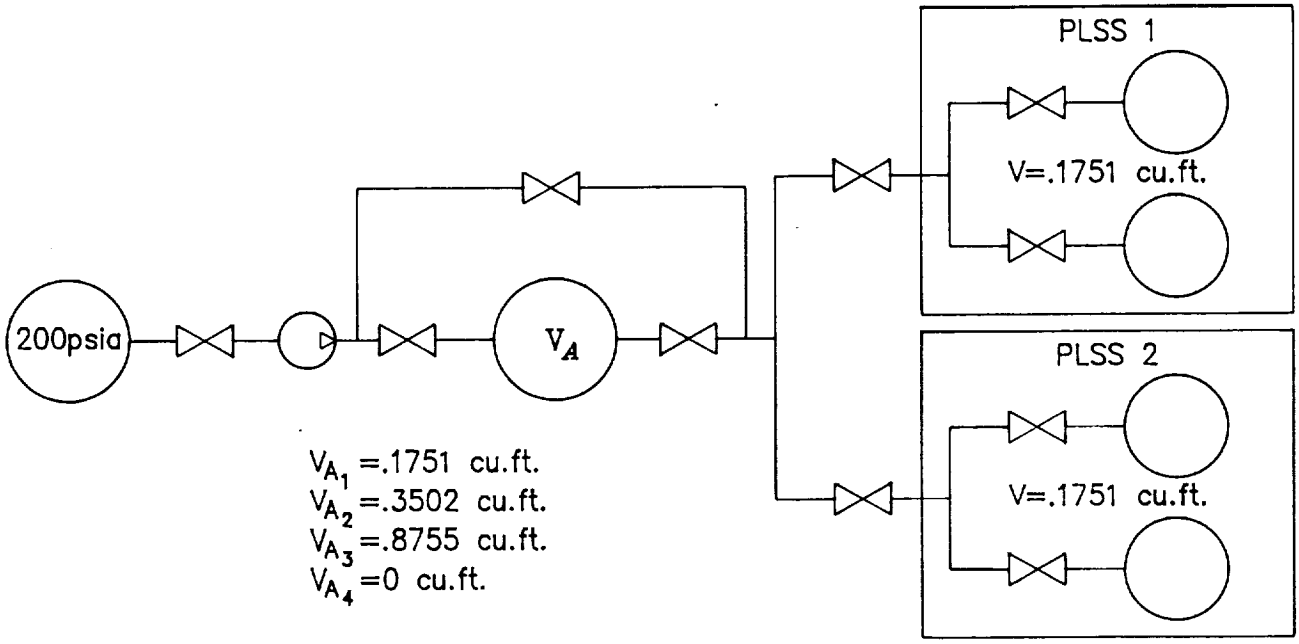

ACCUMULATOR CHARGE

Figure 14 Charging Options

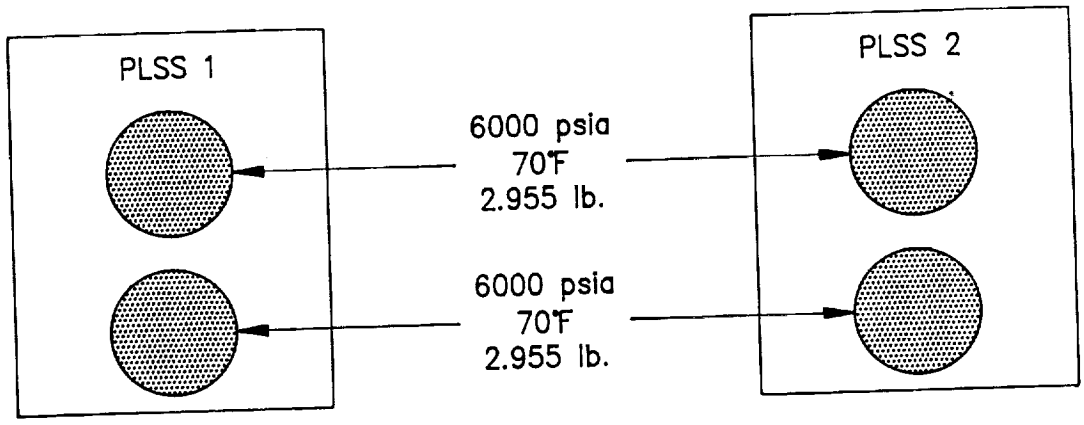

PRIOR TO EVA

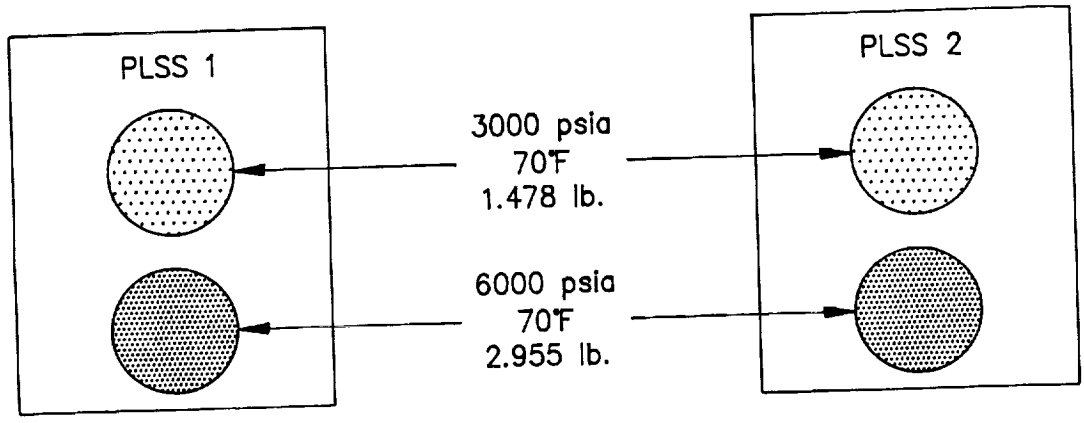

AFTER EVA

(2.955 lb. O_2 CONSUMED)

Figure 15 Standard Normal Usage Assumptions

Table IV

Summary of Significant Parameters with Different Accumulator Sizes

	DIRECT CHARGE	ACCUMULATOR CHARGE		
PLSS O_2TANK VOLUME (cu.ft.) [1]	0.175	0.175	0.175	0.175
ACCUMULATOR VOLUME (cu.ft.)	NA	0.175	0.350	0.876
ACCUMULATOR WEIGHT (lbs) [2]	NA	21	43	107
MAXIMUM CHARGE PRESSURE (psia)	6000	6000	6000	6000
BREATHING TANK OXYGEN @ 6000 psia (lbs)	5.910	5.910	5.910	5.910
ACCUMULATOR OXYGEN @ 6000 psia (lbs)	NA	5.910	11.820	29.550
TOTAL OXYGEN INVENTORY @ 6000 psia (lbs) [3]	11.82	17.73	23.64	41.37
PLSS O_2TANK PRESSURE @ 50% DEPLETION (psia)	3000	3000	3000	3000
EQUILIBRIUM PRESSURE, Pe (psia)	NA	4500	5000	5500
PLSS O_2TANK OXYGEN @ Pe (lbs)	NA	4.433	4.925	5.418
% FULL CHARGE [4]	NA	75	83	92

[1] 2 – PLSS O_2TANKS
[2] K500 MONEL @ SF = 3.0 ON ULTIMATE
[3] 4 PLSS O_2TANKS + ACCUMULATORS
[4] NORMAL USAGE = 2.955 lb.

Table IV summarizes the significant parameters with respect to the various size accumulators and compares them with the direct charge (zero accumulator volume) option. Most of the items are self-explanatory. However, the following should be noted:

1. Accumulator weight was calculated assuming spherical tanks with the thickness established based upon a safety factor of 3 on the ultimate strength (140,000 psi) of K500 Monel. Ten percent was then added to the weight to account for valves and manifolding. It should be further noted that the accumulator weight is independent of the number of tanks used to achieve any given volume.

2. Equilibrium pressure is defined as the pressure that the accumulator and PLSS tanks will reach after they have been connected together assuming the initial (preconnected) pressures were 6000 psia and 3000 psia for the accumulator and PLSS respectively.

5.1 Discussion of Bin Analysis

To determine the time to charge the various size accumulators and the PLSS, and energy consumed during that time, a bin analysis was made using the performance characteristics of each of the four compressor sizes studied. The results are tabulated in Tables V through VIII for each of the compressors analyzed.

The first four columns in each of these tables is simply a tabulation of the data previously given in Figures 5 through 12, i.e. mass flow and power consumption as a function of discharge pressure (or pressure ratio).

The succeeding columns give the incremental charge mass, time, and energy between each pressure increment (500 psi each) for each accumulator size considered. Note that the V = 0.1751 ft^3 is also the volume of two PLSS tanks and is therefore also the case for directly charging (or topping off) the PLSS. The data given at the bottom of each of the tables is the sum of the incremental values for each column above between the pressure ranges within the parenthesis.

Table V

Bin Analysis for 0.75 lb/hr, 5 Hz Compressor

0.75 lb/hr 5hz				V = 0.1751 cu.ft.			V = 0.3502 cu.ft.			V = 0.8755 cu.ft.		
PRESSURE RATIO	P2 (psia)	MASS FLOW (lb/hr)	We (watts)	Mass Chg (lbs)	Time (hrs)	E chg (w-hrs)	Mass Chg (lbs)	Time (hrs)	E chg (w-hrs)	Mass Chg (lbs)	Time (hrs)	E chg (w-hrs)
1.0	200	2.593	17.80	0.197			0.394			0.985		
2.5	500	1.970	40.00	0.295	0.129	3.74	0.591	0.259	7.49	1.477	0.647	18.71
5.0	1000	1.600	54.00	0.492	0.276	12.95	0.985	0.552	25.94	2.462	1.379	64.83
7.5	1500	1.420	61.50	0.492	0.326	18.82	0.985	0.652	37.67	2.462	1.630	94.16
10.0	2000	1.320	66.20	0.492	0.359	22.93	0.985	0.719	45.91	2.462	1.797	114.74
12.5	2500	1.230	69.80	0.492	0.386	26.24	0.985	0.773	52.53	2.462	1.931	131.31
15.0	3000	1.170	72.00	0.492	0.410	29.07	0.985	0.821	58.20	2.462	2.052	145.46
17.5	3500	1.100	73.40	0.492	0.433	31.51	0.985	0.868	63.09	2.462	2.169	157.70
20.0	4000	1.030	74.00	0.492	0.462	34.05	0.985	0.925	68.16	2.462	2.312	170.38
22.5	4500	0.960	74.80	0.492	0.494	36.79	0.985	0.990	73.65	2.462	2.474	184.09
25.0	5000	0.900	75.00	0.492	0.529	39.62	0.985	1.059	79.33	2.462	2.647	198.28
27.5	5500	0.830	75.60	0.492	0.569	42.83	0.985	1.139	85.75	2.462	2.846	214.32
30.0	6000	0.750	76.00	0.492	0.623	47.21	0.985	1.247	94.51	2.462	3.116	236.23
Net change (0-6000 psia)				5.90	5.00	345.76	11.82	10.00	692.22	29.54	25.00	1730.21
Net change (200-6000 psia)				5.71	5.00	345.76	11.43	10.00	692.22	28.56	25.00	1730.21
Net change (3000-6000 psia)				2.95	3.11	232.01	5.91	6.23	464.49	14.77	15.57	1161.00
Net change (4500-6000 psia)				1.48	1.72	129.66	2.96	3.44	259.59	7.39	8.61	648.83
Net change (5000-6000 psia)				0.98	1.19	90.04	1.97	2.39	180.26	4.92	5.96	450.55
Net change (5500-6000 psia)				0.49	0.62	47.21	0.99	1.25	94.51	2.46	3.12	236.23

Table VI

Bin Analysis for 6.0 lb/hr, 32 Hz Compressor

6.0 lb/hr 32hz PRESSURE RATIO	P2 (psia)	MASS FLOW (lb/hr)	We (watts)	V = 0.1751 cu.ft. Mass Chg (lbs)	Time (hrs)	E chg (w-hrs)	V = 0.3502 cu.ft. Mass Chg (lbs)	Time (hrs)	E chg (w-hrs)	V = 0.8755 cu.ft. Mass Chg (lbs)	Time (hrs)	E chg (w-hrs)
1.0	200	11.670	88.90	0.197			0.394			0.985		
2.5	500	9.042	190.38	0.295	0.028	3.98	0.591	0.057	7.97	1.477	0.143	19.92
5.0	1000	7.316	257.69	0.492	0.060	13.48	0.985	0.120	26.98	2.462	0.301	67.44
7.5	1500	6.853	317.31	0.492	0.069	19.97	0.985	0.139	39.97	2.462	0.348	99.91
10.0	2000	7.102	372.70	0.492	0.071	24.33	0.985	0.141	48.70	2.462	0.353	121.73
12.5	2500	7.184	409.15	0.492	0.069	26.93	0.985	0.138	53.91	2.462	0.345	134.74
15.0	3000	7.211	449.52	0.492	0.068	29.35	0.985	0.137	58.76	2.462	0.342	146.86
17.5	3500	7.145	478.65	0.492	0.069	31.81	0.985	0.137	63.68	2.462	0.343	159.18
20.0	4000	7.000	500.00	0.492	0.070	34.04	0.985	0.139	68.15	2.462	0.348	170.34
22.5	4500	6.826	519.23	0.492	0.071	36.27	0.985	0.142	72.61	2.462	0.356	181.49
25.0	5000	6.579	531.73	0.492	0.073	38.57	0.985	0.147	77.22	2.462	0.367	193.02
27.5	5500	6.316	539.80	0.492	0.076	40.88	0.985	0.153	81.85	2.462	0.382	204.58
30.0	6000	6.000	546.00	0.492	0.080	43.38	0.985	0.160	86.84	2.462	0.400	217.05
Net change (0-6000 psia)				5.90	0.80	342.97	11.82	1.61	686.65	29.54	4.03	1716.27
Net change (200-6000 psia)				5.71	0.80	342.97	11.43	1.61	686.65	28.56	4.03	1716.27
Net change (3000-6000 psia)				2.95	0.44	224.95	5.91	0.88	450.36	14.77	2.20	1125.67
Net change (4500-6000 psia)				1.48	0.23	122.83	2.96	0.46	245.91	7.39	1.15	614.66
Net change (5000-6000 psia)				0.98	0.16	84.26	1.97	0.31	168.69	4.92	0.78	421.64
Net change (5500-6000 psia)				0.49	0.08	43.38	0.99	0.16	86.84	2.46	0.40	217.05

Table VII

Bin Analysis for 6.0 lb/hr, 25 Hz Compressor

6.0 lb/hr 25 hz				V = 0.1751 cu.ft.			V = 0.3502 cu.ft.			V = 0.8755 cu.ft.		
PRESSURE RATIO		MASS FLOW (lb/hr)	We (watts)	Mass Chg (lbs)	Time (hrs)	E chg (w-hrs)	Mass Chg (lbs)	Time (hrs)	E chg (w-hrs)	Mass Chg (lbs)	Time (hrs)	E chg (w-hrs)
1.0	200	12.450	98.60	0.197			0.394			0.985		
2.5	500	9.625	196.15	0.295	0.027	3.94	0.591	0.054	7.89	1.477	0.134	19.72
5.0	1000	7.737	255.38	0.492	0.057	12.80	0.985	0.113	25.62	2.462	0.284	64.03
7.5	1500	7.013	309.62	0.492	0.067	18.85	0.985	0.134	37.73	2.462	0.334	94.31
10.0	2000	7.102	359.10	0.492	0.070	23.31	0.985	0.140	46.67	2.462	0.349	116.64
12.5	2500	7.171	396.92	0.492	0.069	26.06	0.985	0.138	52.17	2.462	0.345	130.41
15.0	3000	7.211	434.62	0.492	0.068	28.45	0.985	0.137	56.95	2.462	0.342	142.35
17.5	3500	7.147	465.39	0.492	0.069	30.84	0.985	0.137	61.74	2.462	0.343	154.33
20.0	4000	7.000	488.46	0.492	0.070	33.17	0.985	0.139	66.41	2.462	0.348	166.00
22.5	4500	6.821	506.54	0.492	0.071	35.42	0.985	0.143	70.91	2.462	0.356	177.24
25.0	5000	6.605	517.31	0.492	0.073	37.52	0.985	0.147	75.11	2.462	0.367	187.75
27.5	5500	6.316	526.54	0.492	0.076	39.75	0.985	0.152	79.58	2.462	0.381	198.90
30.0	6000	6.000	531.20	0.492	0.080	42.25	0.985	0.160	84.60	2.462	0.400	211.44
Net change (0-6000 psia)				5.90	0.80	332.35	11.82	1.59	665.38	29.54	3.98	1663.12
Net change (200-6000 psia)				5.71	0.80	332.35	11.43	1.59	665.38	28.56	3.98	1663.12
Net change (3000-6000 psia)				2.95	0.44	218.95	5.91	0.88	438.35	14.77	2.19	1095.66
Net change (4500-6000 psia)				1.48	0.23	119.52	2.96	0.46	239.29	7.39	1.15	598.09
Net change (5000-6000 psia)				0.98	0.16	82.00	1.97	0.31	164.17	4.92	0.78	410.34
Net change (5500-6000 psia)				0.49	0.08	42.25	0.99	0.16	84.60	2.46	0.40	211.44

Table VIII

Bin Analysis for 11.82 lb/hr, 25 Hz Compressor

11.82 lb/hr 25hz				V = 0.1751 cu.ft.			V = 0.3502 cu.ft.			V = 0.8755 cu.ft.		
PRESSURE RATIO	P2 (psia)	MASS FLOW (lb/hr)	We (watts)	Mass Chg (lbs)	Time (hrs)	E chg (w-hrs)	Mass Chg (lbs)	Time (hrs)	E chg (w-hrs)	Mass Chg (lbs)	Time (hrs)	E chg (w-hrs)
1.0	200	24.520	187.80	0.197			0.394			0.985		
2.5	500	18.916	386.54	0.295	0.014	3.90	0.591	0.027	7.81	1.477	0.068	19.53
5.0	1000	15.105	506.15	0.492	0.029	12.91	0.985	0.058	25.85	2.462	0.145	64.60
7.5	1500	13.800	607.69	0.492	0.034	18.96	0.985	0.068	37.96	2.462	0.170	94.87
10.0	2000	13.990	695.80	0.492	0.035	23.08	0.985	0.071	46.20	2.462	0.177	115.48
12.5	2500	14.126	771.92	0.492	0.035	25.68	0.985	0.070	51.42	2.462	0.175	128.52
15.0	3000	14.189	838.46	0.492	0.035	27.98	0.985	0.070	56.02	2.462	0.174	140.02
17.5	3500	14.074	893.85	0.492	0.035	30.16	0.985	0.070	60.37	2.462	0.174	150.90
20.0	4000	13.789	932.30	0.492	0.035	32.25	0.985	0.071	64.56	2.462	0.177	161.36
22.5	4500	13.421	963.46	0.492	0.036	34.28	0.985	0.072	68.63	2.462	0.181	171.53
25.0	5000	12.980	983.85	0.492	0.037	36.29	0.985	0.075	72.65	2.462	0.187	181.59
27.5	5500	12.410	999.96	0.492	0.039	38.44	0.985	0.078	76.96	2.462	0.194	192.36
30.0	6000	11.820	1010.10	0.492	0.041	40.82	0.985	0.081	81.71	2.462	0.203	204.24
Net change (0-6000 psia)				5.90	0.40	324.74	11.82	0.81	650.14	29.54	2.02	1625.02
Net change (200-6000 psia)				5.71	0.40	324.74	11.43	0.81	650.14	28.56	2.02	1625.02
Net change (3000-6000 psia)				2.95	0.22	212.23	5.91	0.45	424.88	14.77	1.12	1061.99
Net change (4500-6000 psia)				1.48	0.12	115.55	2.96	0.23	231.33	7.39	0.58	578.20
Net change (5000-6000 psia)				0.98	0.08	79.26	1.97	0.16	158.67	4.92	0.40	396.61
Net change (5500-6000 psia)				0.49	0.04	40.82	0.99	0.08	81.71	2.46	0.20	204.24

The way in which these tables were constructed is described below using the 11.82 lb/hr compressor as the example (Table VIII). Taking for example the bin between 500 and 1000 psia discharge pressure charging into a 0.1751 tank,

The average mass flow, $\dot{m}$, is $\frac{18.916 + 15.105}{2} = 17.011$ lb/hr

The average power, We, is $\frac{386.59 + 506.15}{2} = 446.35$ watts

The increment of mass, $M = \frac{PV}{RT} = .492$ lbs

where P = pressure increment = 500 psi = 72,000 lb/ft^2

V = tank volume = 0.1751 ft^3

$R = 48.3 \frac{ft\ lb}{lb\ °R}$

T = 70°F = 530°R

Time to charge, t, = $\frac{M}{\dot{m}} = \frac{.492}{17.011} = .029$ hrs

Energy = We(t) = 446.35 x .029 = 12.91 w-hr

To determine the charge mass, time, and energy between any increment larger than 500 psi, one needs simply to sum the incremental values of interest. For example, the totaled values between say 3000 and 6000 psia for the 0.1751 volume case is: charge = 2.95 lb, time = 0.22 hrs, and energy consumed = 212.23 watt hrs as is tabulated in the bottom section of table.

From this example it can be seen how similar analyses can be made for any tank size and any pressure range of interest.

5.2 Summary of Bin Analysis Results

Figure 16 shows the peak power and energy consumed to charge 2.955 lbs of oxygen (one EVA usage) to 6000 psia as a function of compressor size. This plot was constructed from the data given in Tables V through VIII. Again taking the 11.82 lb/hr compressor (Table VIII) as an example, the peak power of 1010 watts

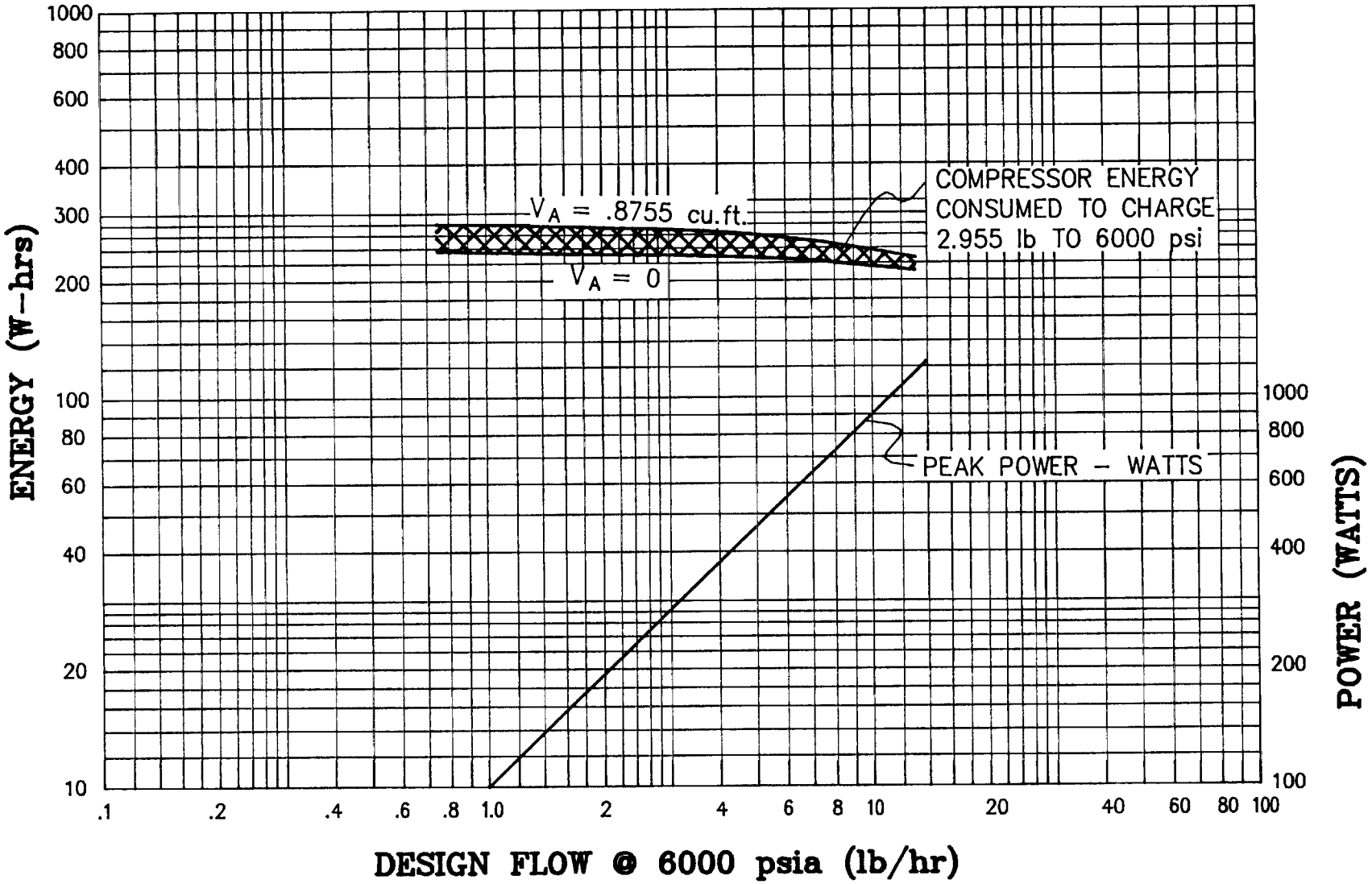

Figure 16 Effect of Design Flow on Electrical Input

occurs at the maximum discharge pressure of 6000 psia. The energy consumed for the direct charge case is 212.23 watt-hrs which is found in Table VIII under the heading V = 0.1751 ft^3 (2 PLSS tanks) with a net change from 3000 to 6000 psia.

For the case where the accumulator volume is 0.8755 ft^3, the energy is the sum of the accumulator charge energy from the equilibrium pressure of 5500 psia to 6000 psia and the PLSS charge energy from 5500 psia to 6000 psia, i.e. 40.82 + 204.24 = 245.06 watt-hrs.

From Figure 16 it is seen that the charge energy drops slightly with increasing compressor size and increases with increasing accumulator volume. Peak power increases almost linearly with compressor size.

Figure 17 summarizes the charge times as a function of compressor size for various charging scenarios. This figure was also constructed using the data contained in Tables V through VIII in a manner similar to that described in the preceding paragraphs.

Shown in Figure 17 are basically three different pieces of information (in addition to the peak power which was previously given in Figure 16). The upper curve indicates the time to direct charge the total 11.82 lbs of oxygen from 200 to 6000 psia into the four PLSS tanks. Below that is a band which covers the range of accumulator sizes from direct charge to the maximum accumulator size of 0.8755 ft^3. The band gives the time to recharge one EVA's oxygen consumption (two astronauts; 2.955 lbs total) vs. compressor design flow. This time is the time required to charge the accumulator from the previously defined equilibrium pressure to 6000 psia plus the time to charge the PLSS from the equilibrium pressure (after precharging with the accumulator) to 6000 psia. The lower curves in Figure 17 indicate the time to top-off the PLSS to 6000 psia after it has been precharged from the various sized accumulators. Obviously, $V_a = 0$ is the special case of the direct charge option.

Figure 17 is useful in that the appropriate compressor/accumulator size options can be evaluated based upon time-to-charge considerations.

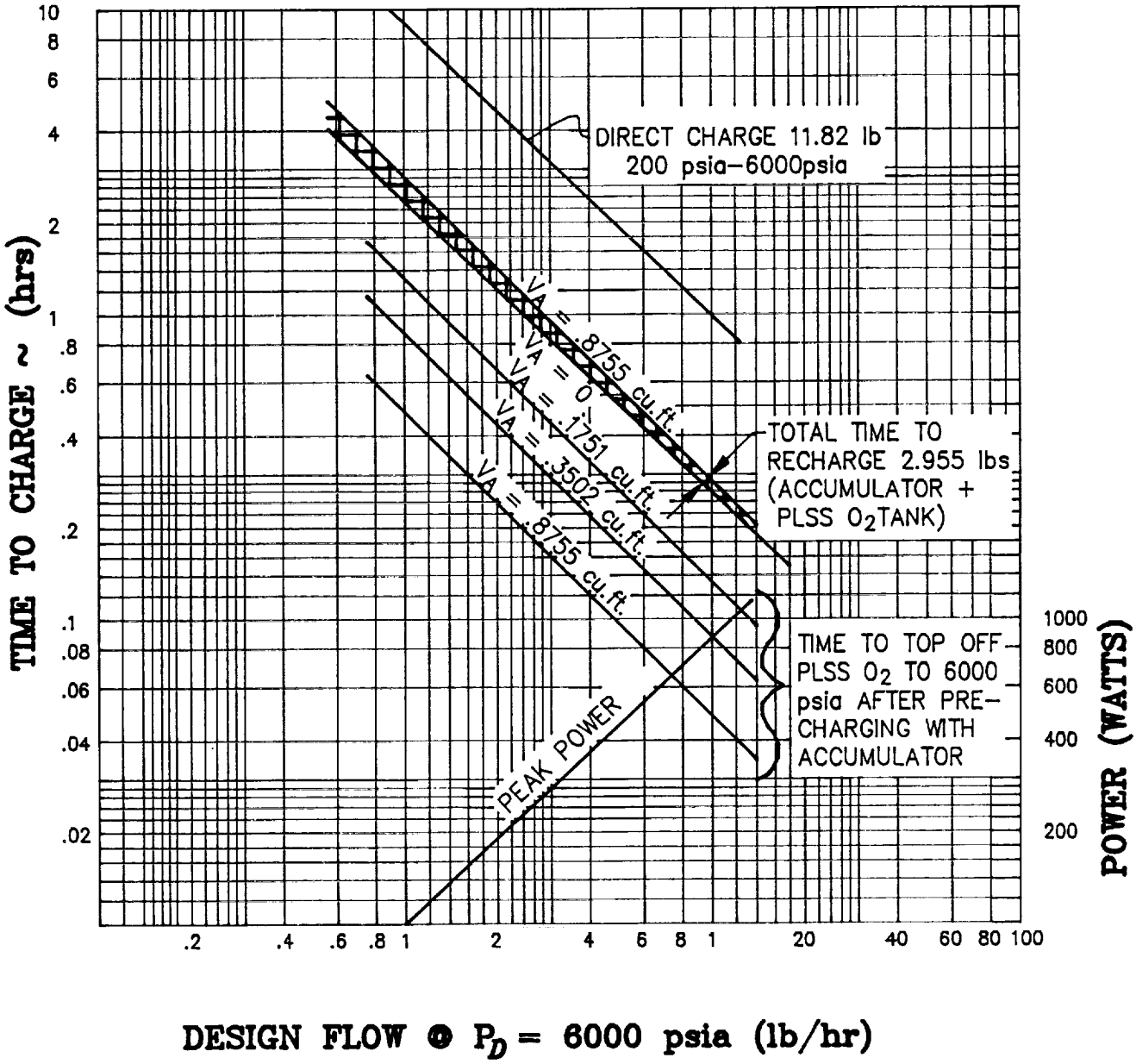

Figure 17 Effect of Design Flow on Charge Time and Power Consumption for Various Accumulator Sizes

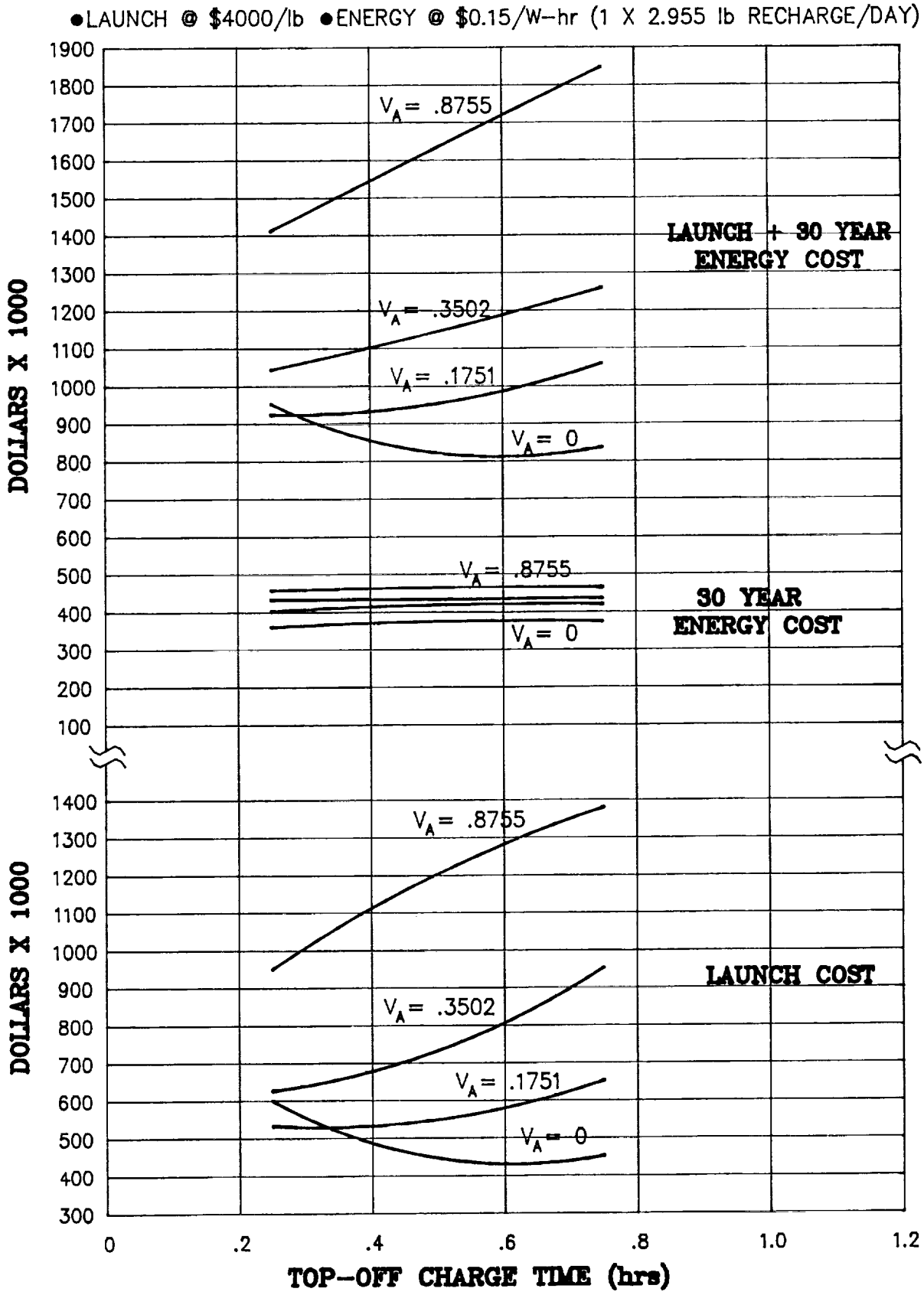

Figure 18 Effect of Top-Off Charge Time on Launch and Energy Cost

Figure 18 summarizes the charge rate study results in terms of launch and energy usage costs as a function of top-off charge time. Top-off charge time was chosen as the basis in this figure since it considers the emergency situation where the astronaut may need to return to an unfinished EVA situation and has little time to await a breathing oxygen recharge. In such a case it is assumed that accumulators, if they are the chosen option, would have been previously charged and the only recharge time of significance is the time to top-off the PLSS to 6000 psia with the compressor.

The cost assumptions used in preparing Figure 18 are that launch cost is $4000 per pound and that energy consumption cost is $0.15 per watt-hour. These values were provided by engineers at NASA-JSC. The launch cost shown in Figure 18 is based upon the sum of the compressor and accumulator weights only. They do not include the weights of dryers, coolers, filters, controls, valves, etc., which should be essentially independent of compressor and accumulator size.

From Figure 18, it is seen that the real driver in terms of cost is weight (i.e. launch cost) and that energy consumption is essentially independent of charge time (energy consumption is computed for compressing 2.955 lb per day for 30 years). Also, the minimum cost is achieved with the direct charge option and the optimum recharge time for the direct charge option is approximately 0.6 hours (36 minutes).

6.0 THERMAL ASPECTS OF CHARGING ACCUMULATOR AND PLSS OXYGEN TANKS

The charge times discussed in the preceding sections were established based upon ideal isothermal conditions. That is, the accumulator and PLSS tanks were assumed to remain at a constant temperature of 70°F during the charging and discharging processes. In reality, however, the oxygen in the tanks (accumulator and PLSS) will heat upon charging as a result of polytropic compression, and the oxygen in the accumulator will cool while discharging into the PLSS due to polytropic expansion. As a result, a finite time will be required to transfer the compression and expansion energies out of, and into, the tanks to reach the desired equilibrium temperature of 70°F (temperature at which theoretical full tank charges, in terms of mass of oxygen, are produced).

Although the definition of the mechanism and rate of the required energy transfer is beyond the scope of this program, ideal analyses assuming no heat transfer into or out of the tanks during the charge/discharge processes were made to quantify the magnitude of this effect. Zero heat transfer was assumed because this represents the worst-case assumption.

Figure 19 schematically shows the energy (heat) transfer required to achieve the ideal 70°F conditions (assuming the initial tank temperatures were at 70°F and that oxygen is delivered from the compressor at 70°F). In charging the tanks, compression energy must be added to the tanks' initial mass of oxygen to raise its pressure to the final state. This compression energy raises the temperature of that initial mass and must be removed by some external means if the final mix temperature is to be at 70°F. Note that no heat need be removed on account of the added oxygen from the compressor because that compression work was done external to the tank.

In discharging the accumulator, the accumulator pressure provides the receiving tank (PLSS) compression energy. At the same time, the loss of energy (expansion) in the accumulator reduces the accumulator oxygen temperature and provides some cooling to the gas received by the PLSS. The remainder of the energy must be externally transferred to the accumulator from the PLSS to achieve the equilibrium temperature of 70°F in both tanks as shown schematically in Figure 19.

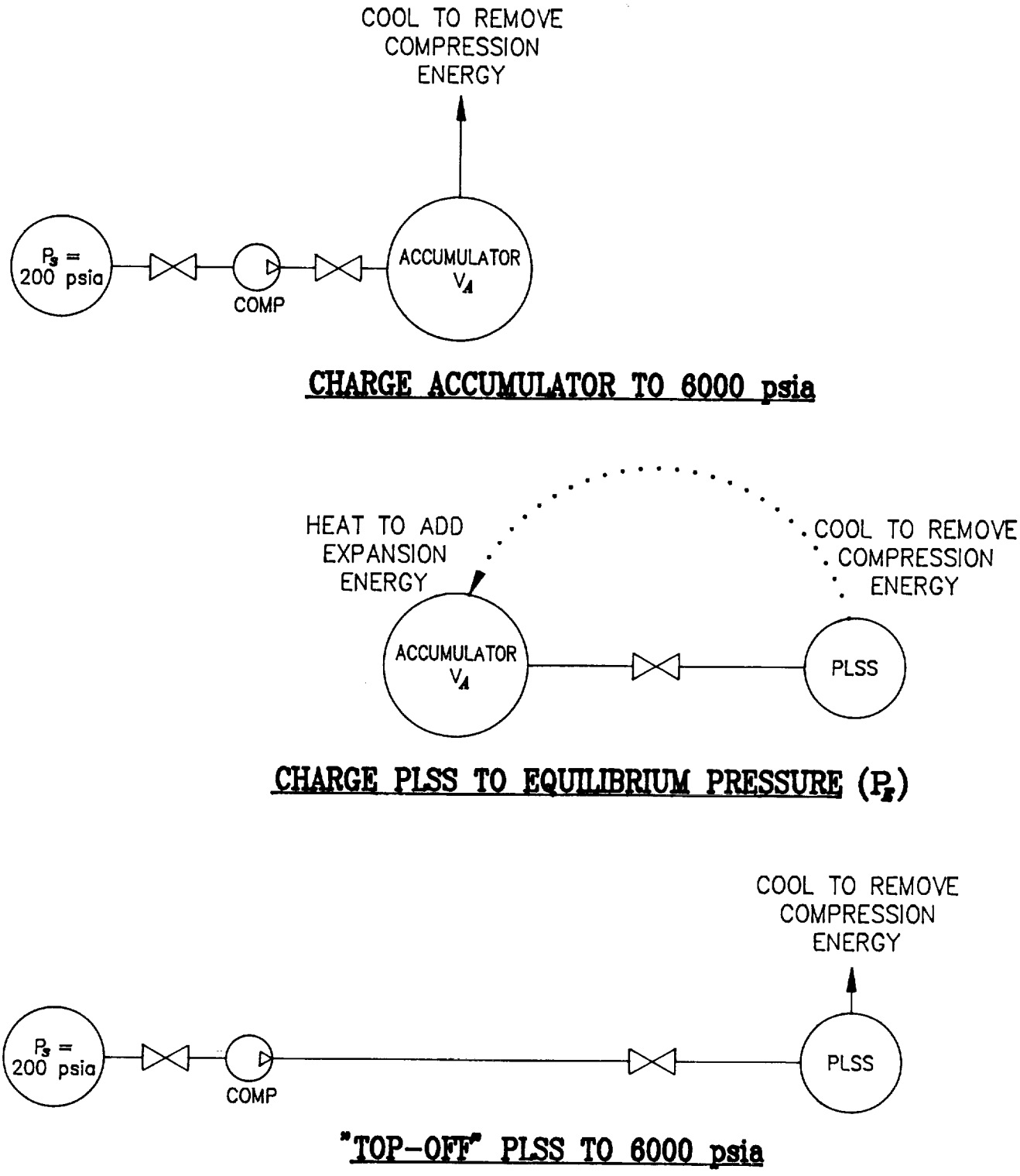

Figure 19 Schematic of Energy Transfer Required to Achieve 70°F Ideal Conditions

For the limiting case analyses conducted, ideal gas properties and the following gas constants were assumed:

$$R = 48.3 \frac{\text{ft-lb}}{\text{lb } ^\circ\text{R}}$$

$$C_p = .217 \frac{\text{BTU}}{\text{lb } ^\circ\text{R}}$$

$$K = \frac{C_p}{C_v} = 1.4$$

Expansion and compression processes were assumed to be reversable adiabatic. The equations used are included in Appendix B.

Figure 20 shows the temperatures that the accumulator and PLSS tanks will reach after discharging the accumulator from 6000 psia into two half-filled (3000 psia) PLSS tanks as a function of accumulator size assuming that there is no external heat energy transfer to or from either tank. The accumulator temperature drop below 530°R (70°F) is seen to decrease as the accumulator size increases. This is because the equilibrium pressure between the two tanks is higher with larger accumulator sizes and the expansion ratio is thus not as great.

The gas temperature in the PLSS, on the other hand, is seen to increase with increasing accumulator size because of the higher compression ratios resulting from the higher equilibrium pressures. Three curves for the PLSS temperature are shown. The lower curve is the temperature at the equilibrium pressure (prior to topping off the PLSS). The middle curve is the temperature after topping off the PLSS to 6000 psi with the compressor (70°F oxygen added). The upper curve is the temperature that would be reached if the PLSS were overpressured (by the compressor) to achieve the full charge mass of 5.91 lb (two PLSS tanks).

Figure 21 shows the equilibrium pressures reached and the PLSS pressure required to reach the full 5.91 lb charge (after charging from the accumulator) as a function of accumulator size. The PLSS pressure is based upon the upper temperature curve shown in Figure 20. It should be noted that the equilibrium pressure between the accumulator and PLSS tanks after connecting them together is

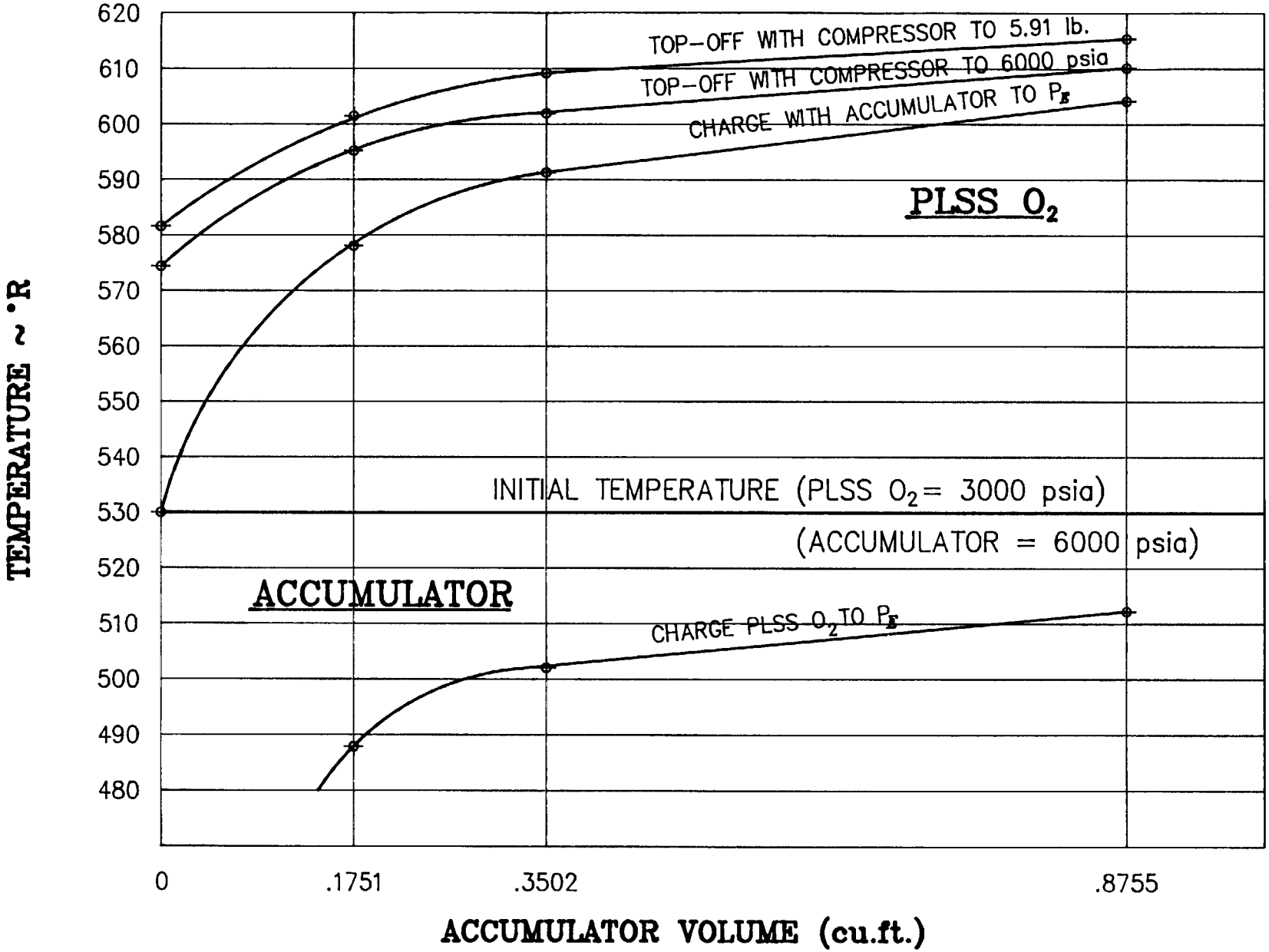

Figure 20 Tank Temperatures with No Energy Transfer

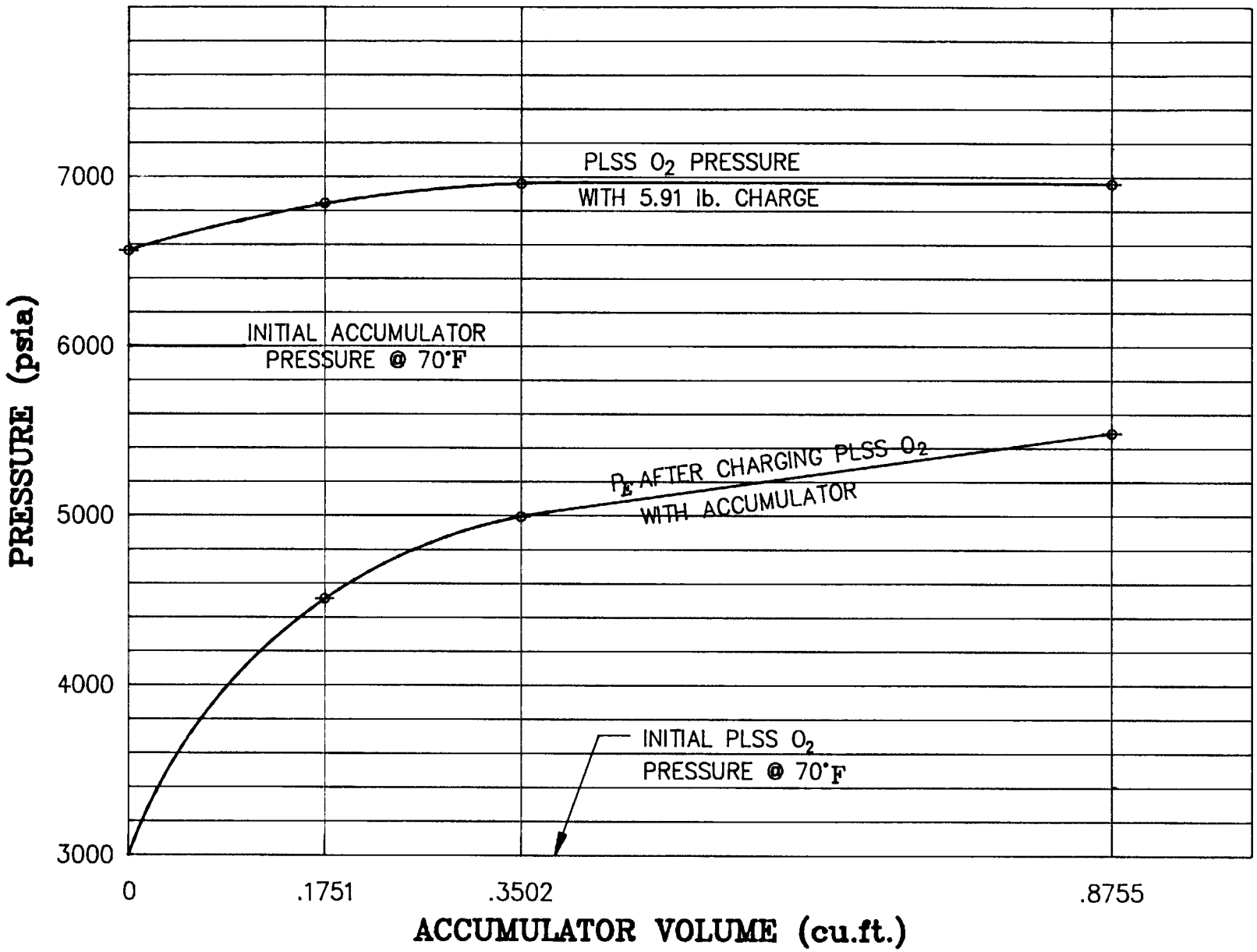

Figure 21 Tank Pressures with No Energy Transfer

independent of the temperatures of either tank. The tank temperatures will however determine the mass of gas contained in each tank.

Figure 22 shows two families of curves for the inventory of gas contained in the PLSS as a function of accumulator volume. The lower two curves (solid and dotted) are the inventory contained after charging the PLSS with the accumulator to the equilibrium pressure. The solid curve is the inventory assuming no heat transfer out of the PLSS and no heat transfer into the accumulator. That is, they are at the temperatures shown in Figure 20. When they are cooled/heated to 70°F, additional oxygen will flow from the accumulator to the PLSS and the PLSS inventory of oxygen will reach the value shown by the lower dotted curve.

If the PLSS is then topped off to 6000 psi by the compressor, it will reach the inventory values shown by the upper family of curves. The solid line assumes that there has been no energy transfer after the accumulator charge process and the PLSS gas temperature is given by the middle PLSS temperature curve shown in Figure 20. The dotted curve assumes that both the accumulator and PLSS had been allowed to reach 70°F prior to the compressor top-off process.

Figure 23 shows the amount of heat energy that must be transferred to achieve the ideal 70°F PLSS full charge conditions after accumulator and compressor top-off charging as a function of accumulator size. The middle curve in the main region of Figure 23 is the heat energy that must be transferred from the PLSS to the accumulator for both to reach 70°F. The lower curve is the heat energy that must be removed from the PLSS during the compressor top-off process to maintain it at 70°F and thus have a full 5.91 lb charge at 6000 psia. The upper curve is the sum of the other two curves and is the total energy that must be removed from the PLSS during the recharging process to achieve a full charge.

It should be noted that zero accumulator volume, shown in Figures 20 through 23, is the equivalent to the direct charge case. From these curves it can be seen that as the accumulator size increases, the PLSS temperature and pressure level required to achieve a full charge also increases. As was stated earlier, the mechanism to accomplish the required energy transfer is beyond the scope of this effort. However, should the direct charge approach be selected, it may be best to side step the energy transfer question by simply increasing the size of the

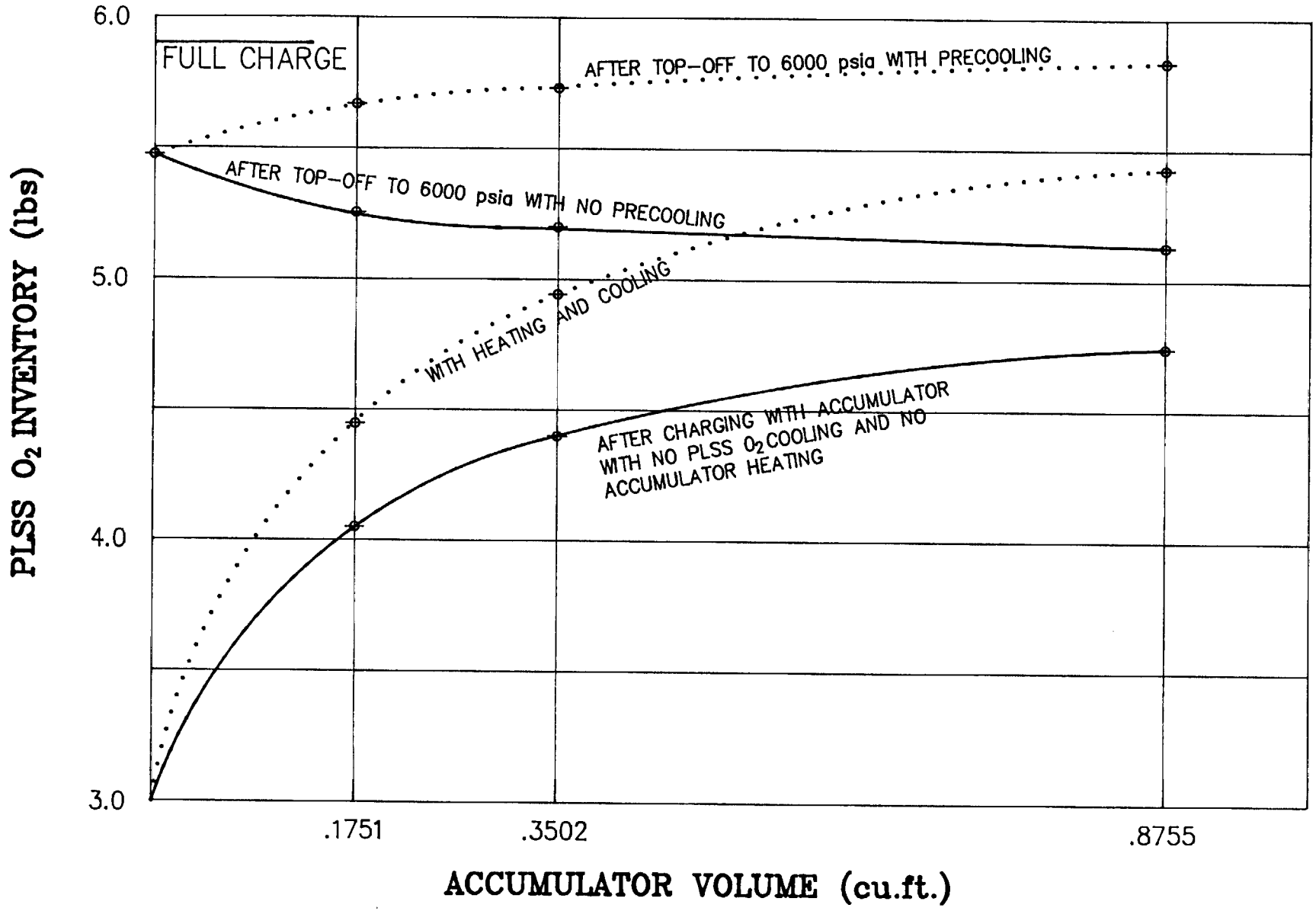

Figure 22 PLSS O_2 Inventory

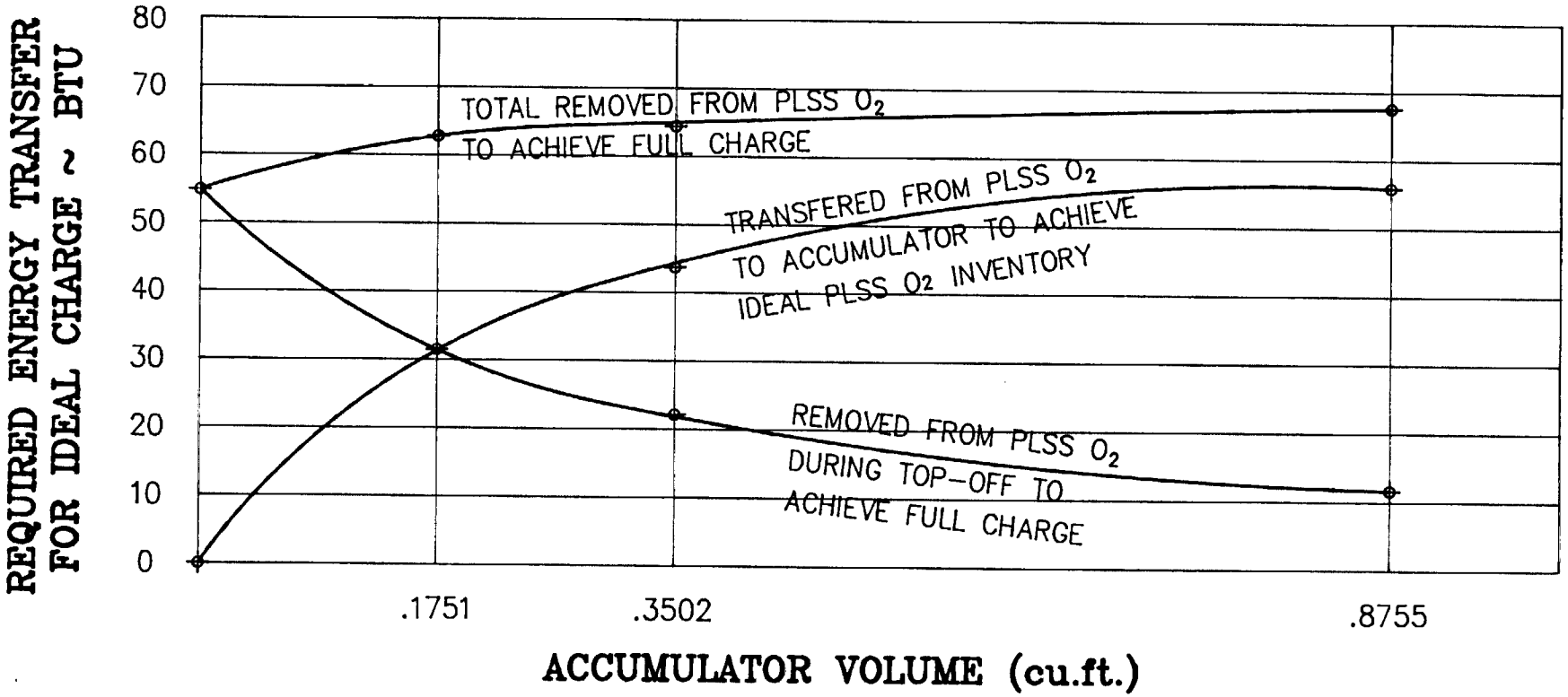

Figure 23 Energy Transfer

PLSS tanks by about 10% such that the defined full inventory of 2.955 lb per tank can be achieved at 6000 psia at a temperature above 70°F. The 70°F equilibrium temperature would then result in a full charge pressure of approximately 5400 psia. When the effects of heat transfer during the charging process are also considered, the required size increase will be less than 10% and the final charge pressure will be somewhat greater than 5400 psi.

APPENDIX A

Appendix A

Effect of Number of Stages on Ideal Adiabatic Power to Pump at the Rate of 11.82 lb/hr

(with Perfect Intercooling Between Stages)

$$P_s = 200 \text{ psia}$$

$$P_d = 6000 \text{ psia}$$

$$\dot{m} = 11.82 \text{ lb/hr}$$

$$\text{Power (Watts)} = \frac{746}{33{,}000} N \left(\frac{K}{K-1}\right)\left(P_s V_s\right)\left[(P_r)^{\frac{K-1}{K}} - 1\right]$$

where: N = Number of Stages

$$K = \frac{C_p}{C_v} = 1.4$$

P_r = Pressure Ratio per Stage

$$P_s = 200 \frac{\text{lb}}{\text{in}^2} = 28{,}800 \frac{\text{lb}}{\text{ft}^2}$$

$$V_s = \frac{\dot{m}\nu_s}{60} = 1.75 \frac{\text{ft}^3}{\text{min}}$$

$$\nu_s = \frac{RT}{P_s} = .889 \frac{\text{ft}^3}{\text{lb}}$$

$$R = 48.3 \frac{\text{ft-lb}}{\text{lb-°R}}$$

$$T = 70°\text{F} = 530°\text{R}$$

$$398.77 \, N \left[(Pr)^{.286} - 1\right]$$

N	P_r	P (Watts)
1	30	655.03
2	5.477	498.95
4	2.340	438.64
6	1.763	420.66
8	1.530	412.03
10	1.405	406.97
20	1.185	397.08

APPENDIX B

Equations Used for Analyses Described in Section 6.0

CHARGING PLSS O_2 TANK FROM PRECHARGED ACCUMULATOR

LIMITING CASE OF NO HEAT TRANSFER FROM (OR TO) EITHER TANK

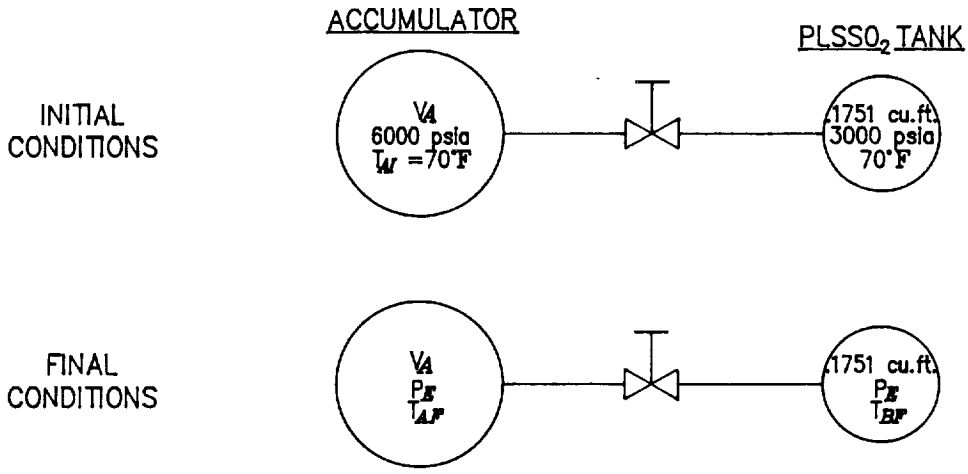

$$M_{AI}T_I + M_{BI}T_I = M_{AF}T_{AF} + M_{BF}T_{BF}$$

$$M_{AI} = \frac{P_{AI}V_A}{RT_I} \qquad M_{BI} = \frac{P_{BI}V_B}{RT_I}$$

$$M_{AF} = \frac{P_{AF}V_A}{RT_{AF}} \qquad M_{BF} = \frac{P_E V_B}{RT_{BF}}$$

$$P_{AI}V_A + P_{BI}V_B = P_E V_A + P_E V_B$$

$$P_E = \frac{P_{AI}V_A + P_{BI}V_B}{V_A + V_B}$$

CHARGING PLSS O_2 TANK FROM PRECHARGED ACCUMULATOR

LIMITING CASE OF NO HEAT TRANSFER FROM (OR TO) EITHER TANK

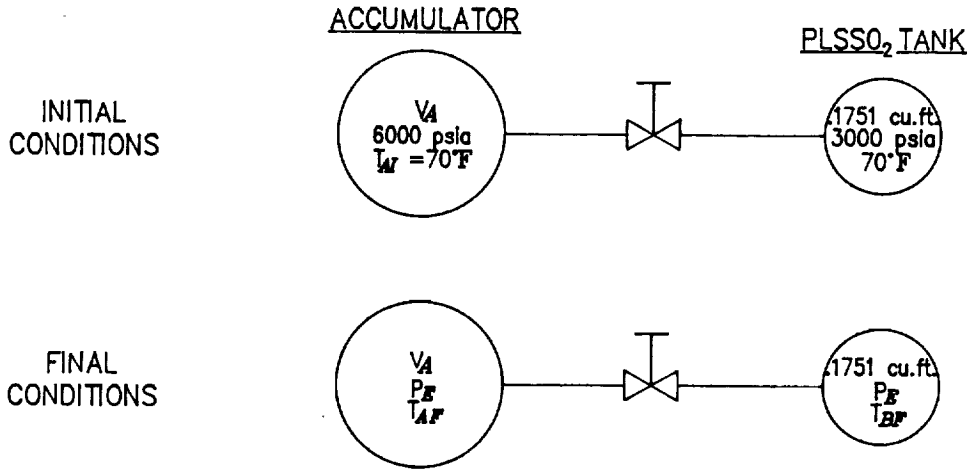

$$M_{AI} = \frac{P_{AI} V_A}{R T_{AI}} \qquad M_{BI} = \frac{P_{BI} V_P}{R T_{AI}}$$

$$H_{AI} = C_P M_A T_{AI} \qquad H_{BI} = C_P M_B T_{BI}$$

$$T_{AF} = T_{AI} \left(\frac{P_{EQ}}{6000}\right)^{\frac{K-1}{K}}$$

$$M_{AF} = \frac{P_E V_A}{R T_{AF}} \qquad M_{BF} = M_T - M_{AF}$$

$$H_{AF} = C_P M_{AF} T_{AF} \qquad H_{BF} = \left[H_{AI} + H_{BI}\right] - H_{AF}$$

$$T_{BF} = \frac{H_{BF}}{C_P M_{BF}}$$

CHARGING PLSS O_2 DIRECTLY

LIMITING CASE OF NO HEAT TRANSFER FROM TANK

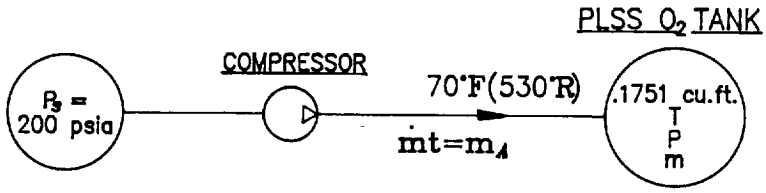

TO SOLVE FOR:
M_F OR P_F
AFTER DEFINING:
P_F OR M_F

$$H_I = M_I C_P T_I$$

$$H_F = H_I + \Delta H_{COMP} + H_A$$

$$H_A = M_A C_P T_A = 530_{mACp}$$

$$\Delta H_{COMP} = M_I C_P T_I \left[\left(\frac{P_F}{P_I} \right)^{\frac{K-1}{K}} - 1 \right]$$

$$M_F = \frac{P_F V_B}{R T_F}$$

OR

$$P_F = \frac{M_F R T_F}{V_B}$$

$$M_F = M_I + M_A$$

TO SOLVE FOR:
ENERGY REMOVAL
TO ACHIEVE 70°F
PLSS O_2 TANK
TEMPERATURE

$$H_R = H_F - H_{70}$$

$$H_R = H_F - M_F C_P 530$$

SUBSCRIPTS:
A = ADDED FROM COMPRESSOR
I = INITIAL
F = FINAL
70 = 70°F